(4) Garrido, L.; Riande, E.; Guzmán, J. *Makromol. Chem., Rapid Commun.* **1983**, *4*, 729.
(5) Flory, P. J. "Statistical Mechanics of Chain Molecules"; Interscience: New York, 1969.
(6) Mark, J. E. *J. Chem. Phys.* **1972**, *56*, 451.
(7) Abe, A. *Polym. J.* **1970**, *1*, 232.
(8) Abe, A. *J. Am. Chem. Soc.* **1968**, *90*, 2205; **1970**, *92*, 1136.
(9) Sutter, U. W.; Flory, P. J. *Macromolecules* **1975**, *8*, 765.
(10) Abe, A.; Hirano, T.; Tsuruta, T. *Macromolecules* **1979**, *12*, 1092.
(11) Allen, G.; Booth, C.; Price, C. *Polymer* **1967**, *8*, 397.
(12) Mark, J. E. *J. Polym. Sci., Polym. Symp.* **1976**, *54*, 91.
(13) Riande, E.; Boileau, S.; Hemery, P.; Mark, J. E. *J. Chem. Phys.* **1979**, *71*, 4206.
(14) Riande, E.; Boileau, S.; Hemery, P.; Mark, J. E. *Macromolecules* **1979**, *12*, 702.
(15) Abe, A. *Macromolecules* **1980**, *13*, 541.
(16) Guggenheim, E. A. *Trans. Faraday Soc.* **1949**, *45*, 714.
(17) Smith, J. W. *Trans. Faraday Soc.* **1950**, *46*, 394.
(18) Marchal, J.; Benoit, H. *J. Polym. Sci.* **1957**, *23*, 223.
(19) Nagai, K.; Ishikawa, T. *Polym. J.* **1971**, *2*, 416.
(20) Doi, M. *Polym. J.* **1972**, *3*, 352.
(21) Liao, S. C., Mark, J. E. *J. Chem. Phys.* **1973**, *59*, 3825.
(22) Flory, P. J. "Principles of Polymer Chemistry"; Cornell University Press: Ithaca, NY, 1953.
(23) Mc Clellan, A. L. "Tables of Experimental Dipole Moments", Vol. I; W. H. Freeman: San Francisco, 1963; Vol. II; Rahara Enterprises: El Cerrito, CA, 1974.
(24) Abe, A.; Mark, J. E. *J. Am. Chem. Soc.* **1976**, *98*, 6468.
(25) Flory, P. J.; Ciferri, A.; Hoeve, C. A. J. *J. Polym. Sci.* **1960**, *45*, 235.
(26) Mark, J. E. *Rubber Chem. Technol.* **1973**, *46*, 593.
(27) Saegusa, T.; Hodaka, H.; Fujii, H. *Polym. J.* **1971**, *2*, 670.
(28) Kops, J.; Larsen, E.; Spanggaard, H. *J. Polym. Sci., Polym. Symp.* **1976**, *56*, 91.
(29) Kops, J.; Hvilsted, S. *Macromolecules*, **1979**, *12*, 889.
(30) Flory, P. J. *Macromolecules*, **1974**, *8*, 381.
(31) Riande, E.; Garcia, M.; Mark, J. E. *J. Polym. Sci., Polym. Phys. Ed.* **1981**, *19*, 1739.
(32) Yamamoto, K.; Kusamizu, S.; Fujita, H. *Makromol. Chem.* **1966**, *19*, 212.
(33) Krigbaum, W. R.; Roe, R. J. *Rubber Chem. Technol.* **1965**, *138*, 1039.
(34) Puett, D. *Makromol. Chem.* **1967**, *100*, 200.
(35) Ishikawa, T.; Nagai, K. *J. Polym. Sci., Polym. Chem. Ed.* **1969**, *7*, 1123.

Theory of Light Scattering and Propagation in Dilute Polymer Solutions: Wormlike Chain Model with Intrinsic and Shape Optical Anisotropies

Mei Hsu Dung and Branka M. Ladanyi*,†

Department of Chemistry, Colorado State University, Fort Collins, Colorado 80523.
Received September 22, 1983

ABSTRACT: We present a continuum model for optical response of dilute solutions of polymer molecules. The solvent is represented as a uniform dielectric continuum. The polymer molecules are modeled as flexible cylinders of constant cross section with a locally axially symmetric anisotropic optical dielectric constant and thus have both permanent and "shape" optical anisotropy. The molecular conformation is represented by the wormlike chain model. Isotropic and depolarized light scattering intensities due to dissolved polymer molecules are evaluated approximately to quadratic order in the scattering wavevector. The refractive index increment of the solution is evaluated as well. The effects on these quantities of molecular shape, size, stiffness, and magnitudes of dielectric tensor components are studied. We show that the local field at a polymer molecule is dependent on the molecular size and conformation. As a consequence of this, familiar expressions, based on the independent scatterer approximation, which relate, for example, isotropic light scattering intensity to the polymer molecular weight and to its mean squared radius of gyration, become inaccurate for some systems. We suggest experiments that may further test the predicted local field effects on light scattering intensities and refractive index increments.

I. Introduction

Our primary goal in this paper is to construct a computationally simple and relatively physically realistic model for the optical response of polymers in dilute solution. Of special interest to us are the local field effects on light scattering (LS) and propagation in these solutions. In most of the treatments of LS from polymer solutions, polymer molecules have been modeled as a collection of independent scatterers.[1] In these models, the effective polarizabilities of the scatterers are scaled to yield the LS intensities close to those observed in a particular solvent, without recourse to a particular local field model. In order to investigate the breakdown of the independent scatterer approximation, it becomes necessary to develop a model for the local field experienced by a polymer molecule in solution. The present paper continues our investigation of models for optical properties of polymers in dilute solution. We have so far considered two types of models for this optical response. One of these is the continuum dielectric model for the polymer–solvent system;[2] the other treats the polymer and the solvent as collections of interacting induced dipoles.[3] This second model is more physically realistic and definitely preferable for solutions of small flexible molecules, but it is impractical for most polymer solutions, for which the model of ref 2 holds more promise. Here we present several improvements and extensions of the work of Ref 2 (from now on referred to as I). In I we developed the general theory of LS and propagation in polymer solutions, where the polymer molecule and the surrounding solvent were modeled as continuous dielectric media. We also presented numerical results for a model in which both the solvent and the polymer molecules were represented as uniform dielectrics with scalar dielectric constants. The polymer was modeled as a flexible cylinder of constant cross section whose conformation was described by the wormlike chain model.[4] We found that this model gave a physically realistic value of the refractive index increment but that the predicted depolarized scattering intensity was too low, since the only

† Alfred P. Sloan Foundation Fellow.

0024-9297/84/2217-1238$01.50/0

source of optical anisotropy in it was the anisotropy in molecular shape. Our goal here is to construct a model that has permanent as well as "shape" optical anisotropy and to investigate its optical response. The specific model we study herein is one where polymer molecules have an optically anisotropic, locally axially symmetric dielectric tensor and are immersed in a uniform dielectric solvent. In I, we considered only LS at essentially zero scattering angle. Here we investigate the dependence of LS intensities on the scattering angle explicitly to the second order in the scattering wavevector.

The paper is organized as follows. In section II, we develop the dielectric theory appropriate to this problem and derive the expressions for the electric field inside a polymer molecule in solution and for the dielectric constant and the LS intensity in terms of this field. In section III we develop an approximate, computationally tractable expression for the field inside a wormlike polymer chain. In section IV we present our results for the dielectric constant and the refractive index increment and in section V for the isotropic and anisotropic LS intensities and their dependence on the scattering wavevector. Our results are summarized and possible extensions of the present work are discussed in section VI.

II. General Dielectric Theory

We consider a dilute solution containing N_p polymer molecules in a container of volume V. The solution is dilute enough so that interactions between different polymer molecules are negligible. The solvent is assumed to be uniform and characterized by a scalar dielectric constant, ϵ_s. In the subsequent development, whenever we mention a dielectric constant or tensor, we will be referring to quantities at optical frequencies, since we will be dealing with light scattering and propagation. The polymer molecules are assumed to be characterized by a local dielectric tensor $\mathbf{D}_p(\mathbf{r})$, where $\mathbf{r}$ denotes a position. We choose $\mathbf{D}_p(\mathbf{r})$ to be an anisotropic, locally axially symmetric tensor. The polymer molecule is assumed to be a flexible cylinder of constant cross section, so that $\mathbf{D}_p$ has the symmetry of the molecule itself. Thus $\mathbf{D}_p$ depends only on the orientation of the local cylinder axis, represented by the unit vector $\hat{u}(\mathbf{r})$, which is tangent to the axis at the point $\mathbf{r}$. $\mathbf{D}_p$ is given by

$$\mathbf{D}_p(\mathbf{r}) = \epsilon_p^0 \mathbf{1} + \Delta\epsilon_p(\hat{u}\hat{u} - \tfrac{1}{3}\mathbf{1}) \tag{2.1}$$

where ϵ_p^0 and $\Delta\epsilon_p$ are, respectively, the isotropic and the anisotropic components of $\mathbf{D}_p$. They are related to $\epsilon_{p\parallel}$ and $\epsilon_{p\perp}$, the components of $\mathbf{D}_p$, respectively, parallel and perpendicular to $\hat{u}$ by

$$\epsilon_p^0 = \tfrac{1}{3}(\epsilon_{p\parallel} + 2\epsilon_{p\perp}) \tag{2.2a}$$

and

$$\Delta\epsilon_p = \epsilon_{p\parallel} - \epsilon_{p\perp} \tag{2.2b}$$

The dielectric tensor, $\mathbf{D}(\mathbf{r})$, at any point $\mathbf{r}$ within the solution has the following properties:

$$\mathbf{D}(\mathbf{r}) = \epsilon_s \mathbf{1} + \Delta(\mathbf{r}) \tag{2.3a}$$

where

$$\Delta(\mathbf{r}) = 0 \qquad \text{for } \mathbf{r} \text{ outside a polymer} \tag{2.3b}$$

and

$$\begin{aligned}\Delta(\mathbf{r}) &= \mathbf{D}_p(\mathbf{r}) - \epsilon_s \mathbf{1} \qquad \text{for } \mathbf{r} \text{ inside a polymer} \\ &= (\epsilon_p^0 - \epsilon_s)\mathbf{1} + \Delta\epsilon_p(\hat{u}\hat{u} - 1/3)\end{aligned} \tag{2.3c}$$

Using Maxwell's equations and the divergence theorem, following the steps outlined in I, the solution for the scalar potential, ψ, may be written as

$$\psi(\mathbf{r}_1) = \psi_0(\mathbf{r}_1) - \frac{1}{4\pi\epsilon_s}\int_w d\mathbf{r}_2\, [\Delta(\mathbf{r}_2)\cdot\nabla_2\psi(\mathbf{r}_2)]\cdot\nabla_2\frac{1}{r_{12}} \tag{2.4}$$

where $\psi_0(\mathbf{r})$ is the potential far away from the polymer and the integral runs only over the volume, w, of a single polymer molecule, since $\Delta(\mathbf{r})$ vanishes when $\mathbf{r}$ is outside a polymer. Using eq 2.3, we find that the above expression becomes

$$\begin{aligned}\psi(\mathbf{r}_1) = \psi_0(\mathbf{r}_1) &- \frac{y_1}{4\pi}\int_w d\mathbf{r}_2\, \nabla_2\psi(\mathbf{r}_2)\cdot\nabla_2\frac{1}{r_{12}} - \\ &\frac{y_2}{4\pi}\int_w d\mathbf{r}_2\, [\hat{u}_2\hat{u}_2\cdot\nabla_2\psi(\mathbf{r}_2)]\cdot\nabla_2\frac{1}{r_{12}}\end{aligned} \tag{2.5}$$

where

$$y_1 = (\epsilon_{p\perp} - \epsilon_s)/\epsilon_s = (\epsilon_p^0 - \epsilon_s - \tfrac{1}{3}\Delta\epsilon_p)/\epsilon_s \tag{2.6a}$$

and

$$y_2 = (\epsilon_{p\parallel} - \epsilon_{p\perp})/\epsilon_s = \Delta\epsilon_p/\epsilon_s \tag{2.6b}$$

The electric field, $\mathbf{E}$, is obtained by taking a gradient of the potential with respect to $\mathbf{r}_1$

$$\begin{aligned}\mathbf{E}(\mathbf{r}_1) = \mathbf{E}_0(\mathbf{r}_1) &+ \frac{y_1}{4\pi}\int_w d\mathbf{r}_2\, [\nabla_2\psi(\mathbf{r}_2)]\cdot\nabla_1\nabla_2\frac{1}{r_{12}} + \\ &\frac{y_2}{4\pi}\int_w d\mathbf{r}_2\, [\hat{u}_2\hat{u}_2\cdot\nabla_2\psi(\mathbf{r}_2)]\cdot\nabla_1\nabla_2\frac{1}{r_{12}}\end{aligned} \tag{2.7}$$

where $\mathbf{E}_0 = -\nabla_1\psi_0$ is the field far away from the polymer. A more convenient form of eq 2.7 is obtained by using the fact that $\nabla_1\nabla_2(1/r_{12}) = -\nabla_2\nabla_2(1/r_{12})$ on the third term on the right-hand side

$$\begin{aligned}\int_w d\mathbf{r}_2\, [\hat{u}_2\hat{u}_2\cdot\nabla_2\psi(\mathbf{r}_2)]\cdot\nabla_1\nabla_2\frac{1}{r_{12}} = \\ \int_w d\mathbf{r}_2 \left[\nabla_2\nabla_2\frac{1}{r_{12}}\cdot\hat{u}_2\hat{u}_2\right]\cdot\mathbf{E}(\mathbf{r}_2)\end{aligned} \tag{2.8}$$

and the chain rule of differentiation and the divergence theorem on the second

$$\int_w d\mathbf{r}_2\, \nabla_2\psi(\mathbf{r}_2)\cdot\nabla_1\nabla_2\frac{1}{r_{12}} = \int_A dA_2\, \frac{\mathbf{r}_{12}\hat{e}_2}{r_{12}^3}\cdot\nabla_2\psi(\mathbf{r}_2) \tag{2.9}$$

Here, $\hat{e}_2$ is an outwardly directed unit vector perpendicular to the surface A of the polymer and $\mathbf{r}_2$ is a position on the polymer surface. Substituting eq 2.8 and 2.9 into eq 2.7, we find that the electric field becomes

$$\begin{aligned}\mathbf{E}(\mathbf{r}_1) = \mathbf{E}_0 &- \frac{y_1}{4\pi}\int_A dA_2\, \frac{\mathbf{r}_{12}\hat{e}_2}{r_{12}^3}\cdot\mathbf{E}(\mathbf{r}_2) + \\ &\frac{y_2}{4\pi}\int_w d\mathbf{r}_2 \left[\nabla_2\nabla_2\frac{1}{r_{12}}\cdot\hat{u}_2\hat{u}_2\right]\cdot\mathbf{E}(\mathbf{r}_2)\end{aligned} \tag{2.10}$$

The above expression is exact and valid for the field at any point $\mathbf{r}_1$ in the solution. We now specialize to the field at a point within the polymer molecule and introduce approximations appropriate to this situation. As can be seen from eq 2.10, $\mathbf{E}$ depends on a set of three coordinates that specify $\mathbf{r}_1$. In the case of a flexible cylinder, it is convenient to choose these to be the local cylindrical coordinate set s_1, ρ_1, and ϕ_1, where s_1 is the distance along the axis, or the arc length, ρ_1 is the cross-section radius, and ϕ_1 is the azimuthal angle. We assume that a good approximation to the field may be obtained by postulating that $\mathbf{E}(\mathbf{r}_1)$ is independent of ρ_1 and ϕ_1 but depends only on s_1.[4] Similarly, $\mathbf{E}(\mathbf{r}_2) \simeq \mathbf{E}(s_2)$. This approximate ex-

pression is obtained by averaging $\mathbf{E}(\mathbf{r}_i)$ over the cross-section variables ρ_i and ϕ_i

$$\mathbf{E}(s_1) = \mathbf{E}_0 + \frac{y_2}{4}a^2\int_0^L ds_2\ \mathbf{Q}_2'(s_1,s_2)\cdot\mathbf{E}(s_2) - \frac{y_1}{2}a\int_0^L ds_2\ \mathbf{Q}_1'(s_1,s_2)\cdot\mathbf{E}(s_2) \quad (2.11)$$

where

$$Q_2'(s_1,s_2) = \left\langle\left(\nabla_2\nabla_2\frac{1}{r_{12}}\right)\cdot\hat{u}_2\hat{u}_2\right\rangle_{\phi_1,\phi_2,\rho_1,\rho_2} = \frac{1}{(\pi a^2)^2}\int_0^a \rho_1\,d\rho_1 \int_0^a \rho_2\,d\rho_2\int_0^{2\pi}d\phi_1\int_0^{2\pi}d\phi_2\left[\nabla_2\nabla_2\frac{1}{r_{12}}\cdot\hat{u}_2\hat{u}_2\right] \quad (2.12)$$

and

$$\mathbf{Q}_1'(s_1,s_2) = \left\langle\frac{\mathbf{r}_{12}\hat{e}_2}{r_{12}^3}\right\rangle_{\phi_1,\phi_2,\rho_1} = \frac{1}{2\pi^2a^2}\int_0^{2\pi}d\phi_1\int_0^{2\pi}d\phi_2\int_0^a \rho_1\,d\rho_1\left[\frac{\mathbf{r}_{12}\hat{e}_2}{r_{12}^3}\right] \quad (2.13)$$

L and a are, respectively, the length and the cross-section radius of the flexible cylinder. $\langle\ldots\rangle_{\phi_1,\phi_2,\rho_1,\rho_2}$ is an average over the cross section at $\mathbf{r}_1$ and $\mathbf{r}_2$. $\langle\ldots\rangle_{\phi_1,\phi_2,\rho_1}$ is an average over the cross section at $\mathbf{r}_1$ and the azimuthal angle at $\mathbf{r}_2$. In eq 2.13, where this average is used, ρ_2 is on the surface of the polymer molecule.

Equation 2.11 is further simplified by assuming that the dependence of the field on s_i is weak. This is motivated by the fact that the field is constant inside several simple rigid objects, such as spheres, ellipsoids, and infinite cylinders, with isotropic or anisotropic $\mathbf{D}_p$. Thus, to the lowest order of approximation, we assume that $\mathbf{E}(s_2) \cong \mathbf{E}(s_1)$ and replace $\mathbf{E}(s_2)$ with $\mathbf{E}(s_1)$ in eq 2.12 and 2.13. This allows us to obtain a first-order expression for $\mathbf{E}(s_1)$ in terms of $\mathbf{E}_0$

$$\mathbf{E}(s_1) = \mathbf{G}(s_1)\cdot\mathbf{E}_0 \quad (2.14)$$

where

$$\mathbf{G}(s_1) = [1 + \mathbf{H}]^{-1} \quad (2.15)$$

with

$$\mathbf{H}(s_1) = \int_0^L ds_2\ \mathbf{H}'(s_1,s_2) \quad (2.16)$$

and

$$\mathbf{H}'(s_1,s_2) = y_1\frac{a}{2}\mathbf{Q}_1'(s_1,s_2) - y_2\frac{a^2}{4}\mathbf{Q}_2'(s_1,s_2) \quad (2.17)$$

Equation 2.14 is the central result of this section. It was shown in I that the solution dielectric constant and the LS intensity expressions depend on the molecular conformation only through $\mathbf{G}$. In particular, the solution dielectric constant, ϵ, is given by

$$\epsilon = \frac{1}{3}\mathrm{Tr}\,\langle\mathbf{D}\rangle = \epsilon_s + \frac{c}{3}\int_w d\mathbf{r}\ \mathrm{Tr}\,\langle(\mathbf{D}_p(\mathbf{r}) - \epsilon_s\mathbf{1})\cdot\mathbf{G}(\mathbf{r})\rangle \quad (2.18)$$

where

$$c = N_p/V \quad (2.19)$$

is the polymer concentration, Tr is a trace of a tensor, and $\langle\ldots\rangle$ denotes an equilibrium ensemble average. The LS intensity, I_{fi}, at $\mathbf{r}_0$ is the average of the square of the magnitude of fluctuating scattered field, $\mathbf{E}_{sc}$, polarized along $\hat{n}_f$, given that the incident field (in the present case, $\mathbf{E}_0$) is polarized along $\hat{n}_i$[1a,2]

$$I_{fi} = \langle|\hat{n}_f\cdot\mathbf{E}_{sc}|^2\rangle \quad (2.20)$$

$$= \frac{k_0^4c|\langle\mathbf{E}\rangle|^2}{[(4\pi)^2r_0]^2}\int_w d\mathbf{r}\int_w d\mathbf{r}'\ \hat{n}_f\cdot\langle(\mathbf{D}_p(\mathbf{r}) - \epsilon_s\mathbf{1})\cdot\mathbf{G}(\mathbf{r})\cdot\hat{n}_i \times \hat{n}_i\cdot\mathbf{G}^\dagger(\mathbf{r}')\cdot(\mathbf{D}_p(\mathbf{r}') - \epsilon_s\mathbf{1})\rangle\cdot\hat{n}_f\exp(i\mathbf{q}\cdot(\mathbf{r} - \mathbf{r}')) \quad (2.21)$$

where k_0 is the wavevector in the vacuum, $k = nk_0$ is the wavevector in the medium, and $\mathbf{G}^\dagger$ is the Hermitian conjugate of $\mathbf{G}$. n is the refractive index, given by

$$n^2 = \epsilon \quad (2.22)$$

$\mathbf{q}$ is the difference between the scattered wavevector $\mathbf{k}_f$ and the incident wavevector $\mathbf{k}_i$

$$\mathbf{q} = \mathbf{k}_f - \mathbf{k}_i \quad (2.23)$$

The scattering is assumed to be quasi-elastic, so that

$$|k_f| = |k_i| = k \quad (2.24)$$

Note that only LS due to polymers is possible in our model, since the solvent is assumed to be a uniform dielectric. This is never the case for real systems, where the LS intensity due to the pure solvent needs to be subtracted in order to get the solute contribution to this quantity. However, this approximation is quite reasonable for evaluating the local field contribution to LS from optically anisotropic molecules.

$\mathbf{G}$ depends on the molecular conformation in a complicated way, namely through $(1 + \mathbf{H})^{-1}$, where $\mathbf{H}$ is a conformation-dependent quantity. For a flexible polymer it is impossible to derive an expression for $\mathbf{G}$ that would be exact as well as computationally tractable. Reasonable approximations to $\mathbf{G}$ may be obtained in two situations: (1) the dielectric tensors of the polymer and the solvent are similar in magnitude, so that both y_1 and y_2 are small and a series expansion of $\mathbf{G}$ in y_1 and y_2 converges rapidly; (2) the polymer chain is stiff, so that $\mathbf{H}$ is close to $\langle\mathbf{H}\rangle_{\hat{u}_1}$, its average over $\hat{u}_2$ and the distance $\mathbf{R}_{12}$ between cross-section centers at $\mathbf{r}_1$ and $\mathbf{r}_2$. In this latter case $\mathbf{H}$ can be expanded around this average value

$$\mathbf{H}(s_1) = \langle\mathbf{H}(s_1)\rangle_{\hat{u}_1} + \Delta\mathbf{H}(s_1) \quad (2.25)$$

$\Delta\mathbf{H}$ is small, so that a good approximation to $\mathbf{G}$ is obtained by neglecting its contribution

$$\mathbf{G} \cong \mathbf{G}_a \cong (1 + \langle\mathbf{H}\rangle_{\hat{u}_1})^{-1} \quad (2.26)$$

In the following section, we will derive an explicit expression for $\mathbf{G}_a$ for the wormlike model of polymer chain conformation.

III. Electric Field inside a Wormlike Polymer

In this section we evaluate $\mathbf{G}_a$ for a wormlike chain model of a polymer molecule. Our methods are similar to those used in I but differ from them in that the anisotropic component, proportional to y_2 is now present. Also, for reasons of consistency, we evaluate the coefficient of y_1 by averaging over ρ_1, instead of assuming that ρ_1 is on the polymer surface, as we did in I.

We consider a wormlike polymer of length L and radius a. A position $\mathbf{r}_i$ inside the polymer is expressed in terms of $\mathbf{R}_i$, the position on the axis, and $\rho_i = \rho_i\hat{e}_i$, the distance between the axis and the cross-section location

$$\mathbf{r}_i = \mathbf{R}_i + \rho_i\hat{e}_i \quad (3.1)$$

The distance $\mathbf{R}_i$ is a function of the arc length s_i and the

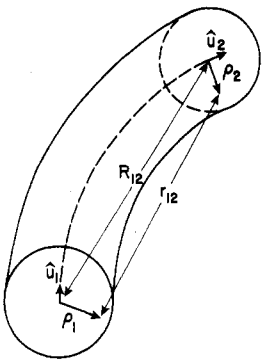

Figure 1. Polymer molecule section displaying distance $\mathbf{r}_{12}$, radial vectors ρ_1 and ρ_2, tangential unit vectors $\hat{u}_1$ and $\hat{u}_2$, and center-to-center distance $\mathbf{R}_{12}$.

tangential unit vector $\hat{u}_i = \hat{u}(s_i)$. For example, $\mathbf{R}_{12}$ can be written as

$$\mathbf{R}_{12} = \int_{s_1}^{s_2} ds\ \hat{u}(s) \tag{3.2}$$

A section of the flexible cylindrical molecule, with all the relevant distances and unit vectors displayed, is depicted in Figure 1.

In order to evaluate $\langle \mathbf{H}(s_1) \rangle_{\hat{u}_1}$, we need a probability distribution function of $\hat{u}_2$, $s = |s_2 - s_1|$, and $\mathbf{R}_{12}$ for a fixed $\hat{u}_1$. As was pointed out in I, such a distribution exists for the wormlike chain only in two limiting cases: (1) $s \ll 1/2\lambda$ (where $1/2\lambda$ is the persistence length[1b]); and (2) in the opposite extreme, $s \gg 1/2\lambda$. In the first case, the molecular shape is that of a straight cylinder, so that the molecule possesses only a single conformation. In the second case, the molecule is very flexible on the distance scale considered, so that a Gaussian distribution is applicable, to a good approximation.[1b] The corrections to the Gaussian distribution are expressed as an expansion in powers of $1/\lambda s$. No satisfactory expression exists in the intermediate range of λs values. We note, however, that extending the region 1 to somewhat flexible cylinders is quite feasible and would be desirable for the present and similar problems. Work on this problem is in progress.[5]

The average over $\hat{u}_2$ and $\mathbf{R}_{12}$ of $\mathbf{H}'(s_1,s_2)$, defined in eq 2.16, is a function only of s. Depending on the value of s, $\langle \mathbf{H}' \rangle_{\hat{u}_1}$ will be given by its value in region 1, which we denote by the subscript "c" (meaning "cylinder") or its value in region 2, which we denote by "d" (meaning "dipolar"). Thus we have

$$\langle \mathbf{H}'(s) \rangle_{\hat{u}_1} = \mathbf{H}_c'(s) \qquad \text{for } s \le b/2\lambda \tag{3.3a}$$

and

$$\langle \mathbf{H}'(s) \rangle_{\hat{u}_1} = \langle \mathbf{H}_d'(s) \rangle_{\hat{u}_1} \qquad \text{for } s > b/2\lambda \tag{3.3b}$$

where b is a number of order unity. In the first region no averaging of $\mathbf{H}'$ is necessary, given that the molecule has a unique conformation.

A. Contribution to the Field from Region 1. In the case of a straight cylinder, we choose the cylinder axis to be the z axis in the molecular frame. The vectors $\hat{u}_i$ are then all equal to $\hat{k}$, the unit vector along z, while $\hat{e}_i$, $\mathbf{r}_{12}$, and r_{12}^2 may be written as

$$\hat{e}_i = \cos \phi_i \hat{i} + \sin \phi_i \hat{j} \tag{3.4}$$

$$\mathbf{r}_{12} = (\rho_2 \cos \phi_2 - \rho_1 \cos \phi_1)\hat{i} + (\rho_2 \sin \phi_2 - \rho_1 \sin \phi_1)\hat{j} + (s_2 - s_1)\hat{k} \tag{3.5}$$

and

$$r_{12}^2 = \rho_1^2 + \rho_2^2 - 2\rho_1\rho_2 \cos(\phi_1 - \phi_2) + (s_1 - s_2)^2 \tag{3.6}$$

where $\hat{i}$ and $\hat{j}$ are, respectively, unit vectors along x and y molecule-fixed axes. $\mathbf{H}_c'$ is

$$\mathbf{H}_c'(s) = \frac{y_1 a}{2}\mathbf{Q}_{1c}'(s) - y_2\frac{a^2}{4}\mathbf{Q}_{2c}'(s) \tag{3.7}$$

where $\mathbf{Q}_{1c}'$ and $\mathbf{Q}_{2c}'$ are given by eq 2.13 and 2.12. Explicit expressions for them in the cylinder case are obtained by using eq 3.4 to 3.6. Given that r_{12} depends only on $\phi = \phi_1 - \phi_2$, we change the angular averages from the (ϕ_1, ϕ_2) set to the (ϕ, ϕ_2) set. The average over ϕ_2 can then be done analytically, with the result

$$\mathbf{Q}_{1c}' = \left\langle \frac{\mathbf{r}_{12}\hat{e}_2}{r_{12}^3} \right\rangle_{\phi,\phi_2,\rho_1} = \frac{1 - \hat{u}_1\hat{u}_1}{2\pi a^2}\int_0^{2\pi} d\phi \int_0^a d\rho_1\ \rho_1 \frac{a - \rho_1 \cos\phi}{[\rho_1^2 + a^2 - 2a\rho_1 \cos\phi + s^2]^{3/2}} \tag{3.8}$$

and

$$\mathbf{Q}_{2c}' = \left\langle \left(\nabla_2\nabla_2 \frac{1}{r_{12}} \right) \cdot \hat{u}_2\hat{u}_2 \right\rangle_{\phi,\phi_2,\rho_1,\rho_2} = \left\langle \frac{(3\mathbf{r}_{12}\mathbf{r}_{12} - 1r_{12}^2)\cdot\hat{u}_2\hat{u}_2}{r_{12}^5} \right\rangle_{\phi,\phi_2,\rho_1,\rho_2} = \frac{2\hat{u}_1\hat{u}_1}{\pi a^4}\int_0^{2\pi} d\phi \int_0^a \rho_1\, d\rho_1 \int_0^a \rho_2\, d\rho_2\, \frac{3s^2 - r_{12}^2}{r_{12}^5} \tag{3.9}$$

In order to evaluate $\mathbf{H}$ itself, we need integrals of $\mathbf{Q}_{1c}'$ and $\mathbf{Q}_{2c}'$ over s from $s = 0$ to $s = s'$, where the value of s' is determined by the location of s_1. Thus we define $q_{1c}(s')$ and $q_{2c}(s')$ by

$$\int_0^{s'} ds\ \mathbf{Q}_{1c}'(s) = (1 - \hat{u}_1\hat{u}_1)q_{1c}(s') \tag{3.10}$$

and

$$\int_0^{s'} ds\ \mathbf{Q}_{2c}'(s) = \hat{u}_1\hat{u}_1 q_{2c}(s') \tag{3.11}$$

Integrations over s and ϕ in q_{1c} can be carried out analytically, with the result

$$q_{1c}(s') = \frac{1}{\pi a^3}\int_0^a \rho_1\, d\rho_1\, F(\rho_1,s') \tag{3.12}$$

where $F(\rho_1,s')$ is given by

$$F(\rho,s') = \frac{s'}{[(\rho_1 + a)^2 + s'^2]^{1/2}} \times \left[K(m) + \frac{a - \rho_1}{a + \rho_1}\Pi\left(\frac{\pi}{2}, \frac{-4a\rho_1}{(\rho_1 + a)^2}, m \right) \right] \tag{3.13}$$

K is the complete elliptic integral of the first kind[6] and Π the elliptic integral of the third kind.[6] m is defined as

$$m = 2\left[\frac{a\rho_1}{(a + \rho_1)^2 + s'^2} \right]^{1/2} \tag{3.14}$$

Similarly, the integrals over ρ_1, ρ_2, and s in q_{2c} can be done analytically, with the result

$$q_{2c}(s') = \frac{4}{\pi a^4}\int_0^{\pi} d\phi\ T(\cos\phi, s') \tag{3.15}$$

where $T(c,s)$ is given by

$$T(c,s) = \frac{s}{1-c^2}\{[2a^2(1-c)+s^2]^{1/2} - 2[a^2+s^2]^{1/2} + s\} + \frac{cs^2}{(1-c^2)^{3/2}}\left\{\arctan\left[\frac{s^2c + a^2(1-c^2)}{s[(1-c^2)(2a^2(1-c)+s^2)]^{1/2}}\right] - \arctan\frac{[1-c^2]^{1/2}}{c} - \arctan\left[\frac{sc}{[(1-c^2)(a^2+s^2)]^{1/2}}\right] + \arctan\left[\frac{[(1-c^2)(a^2+s^2)]^{1/2}}{sc}\right]\right\} \quad (3.16)$$

away from $c = \pm 1$. $T(-1,s)$ and $T(1,s)$ are derived in Appendix A and are given, respectively, by eq A.7 and A.1. The remaining integrations in eq 3.12 and 3.15 have to be done numerically. As stated earlier, q_{1c} has already been evaluated in I, using the approximation $\rho_1 = a$. We evaluated it here removing his approximation. We found that the new and the old values gave essentially the same results for all the measurable quantities we evaluated, although the two expressions for $q_{1c}(s)$ differ at small values of s. This fact confirms the validity of the approximation to the field inside a molecule we developed in section II, namely that $\mathbf{E}(\mathbf{r}_i) \cong \mathbf{E}(s_i)$. The field is indeed weakly dependent on the cross-section vector.

When s' becomes large, i.e. when $s' \gg a$, q_{1c} and q_{2c} can be expanded in powers of a/s', with the result

$$q_{1c}(s') = \frac{1}{a}\left[\frac{1}{2} - \frac{1}{4}\left(\frac{a}{s'}\right)^2 + \frac{3}{8}\left(\frac{a}{s'}\right)^4 + \dots\right] \quad (3.17)$$

and

$$q_{2c}(s') = \frac{1}{a^2}\left[-\left(\frac{a}{s'}\right)^2 + \frac{3}{2}\left(\frac{a}{s'}\right)^4 - \dots\right] \quad (3.18)$$

From the above equations it can be seen that at large s', the contribution of q_{2c} to $\mathbf{H}$ becomes negligible relative to that of q_{1c}. $\mathbf{Q}_{2c}'$ has an integrable singularity at the origin, $\mathbf{r}_{12} = 0$. As a result of this, q_{2c} is finite at $s' = 0$. It is shown in Appendix A that the values of q_{1c} and q_{2c} at $s' = 0$ are

$$q_{1c}(0) = 0 \quad (3.19)$$

and

$$q_{2c}(0) = -2/a^2 \quad (3.20)$$

This value of $q_{1c}(0)$ differs from the one obtained in I, namely $q_{1c}(0) \cong 1/4a$. The reasons for this difference are explained in Appendix A.

B. Contribution to the Field from Region 2. When s becomes large compared to the persistence length $1/2\lambda$, the molecular radius, a, becomes small compared to R_{12}, the distance along the backbone, for most of the likely polymer conformations. Thus we may expand eq 2.12 and 2.13 in powers of a/R_{12} and obtain

$$\mathbf{Q}_1' \cong \frac{a}{2R_{12}^3}(1 - 3\hat{R}_{12}\hat{R}_{12})\cdot(1 - \hat{u}_2\hat{u}_2) \equiv \mathbf{Q}_{1d}' \quad (3.21)$$

and

$$\mathbf{Q}_2' \cong \frac{1}{R_{12}^3}(3\hat{R}_{12}\hat{R}_{12} - 1)\cdot\hat{u}_2\hat{u}_2 \equiv \mathbf{Q}_{2d}' \quad (3.22)$$

Here we have assumed that $\hat{e}_1$ and $\hat{e}_2$ are uncorrelated. We note that $\mathbf{Q}_1'$ and $\mathbf{Q}_2'$ now depend on a dipole tensor interaction of the axial distance $\mathbf{R}_{12}$—hence the name "dipolar" for the contribution to the field from this region.

Since the points 1 and 2 correspond now to a large value of s, we use the probability distribution valid for $\lambda s \gg 1$ to average over $\mathbf{R}_{12}$ and $\hat{u}_2$ for a fixed $\hat{u}_1$. In this range of s values, the distribution is approximately Gaussian. The deviations from Gaussian behavior may be expanded in powers of $1/\lambda s$. This distribution has been derived by Gobush et al.[7] and has the form

$$f = \frac{1}{(4\pi)^{1/2}}\left(\frac{3}{2\pi\lambda s}\right)^{3/2} \times \exp\left(-\frac{3R^2}{2\lambda s}\right)\sum_{l=0}^{\infty}\sum_{m=-l}^{l} Y_{l,m}(\theta,\phi')\, F_l^{|m|}(R,\theta_R) \quad (3.23)$$

where $\mathbf{R} = \mathbf{R}_{12}$, $\cos\theta_R = \hat{u}_1\cdot\hat{R}$, $\cos\theta = \hat{u}_1\cdot\hat{u}_2$, ϕ' is the relative azimuthal angle between $\hat{u}_2$ and $\mathbf{R}$, Y_{lm}'s are spherical harmonics, and $F_l^{|m|}$'s are given in ref 7b. Using the above distribution, we obtain the following results for the averages of $\mathbf{Q}_{1d}'$ and $\mathbf{Q}_{2d}'$:

$$\langle\mathbf{Q}_{1d}'\rangle_{\hat{u}_1} = \frac{3a\lambda^3}{25}\left(\frac{3}{2\pi t^5}\right)^{1/2}\left[\left(1 - \frac{743}{630t} + \frac{x_1}{t^2}\right)\mathbf{1} - \left(\frac{20}{9} - \frac{2257}{420t} + \frac{z_1}{t^2}\hat{u}_1\hat{u}_1\right)\right] \quad (3.24)$$

and

$$\langle\mathbf{Q}_{2d}'\rangle_{\hat{u}_1} = \frac{\lambda^3}{25}\left(\frac{3}{2\pi t^5}\right)^{1/2}\left[\left(1 - \frac{221}{60t} + \frac{x_2}{t^2}\right)\mathbf{1} + \left(\frac{5}{3} + \frac{3089}{140t} + \frac{z_2}{t^2}\right)\hat{u}_1\hat{u}_1\right] \quad (3.25)$$

where $t = \lambda s$. The values of x_1, x_2, z_1, and z_2 are not determined by the above equations. They are obtained below by requiring that $\langle H'\rangle_{\hat{u}_1}$ be continuous at $s = b/2\lambda$.

C. Connection between Regions 1 and 2. When $\lambda s \cong 1$, neither of the two limiting cases discussed above applies. There is at present no distribution function f valid for this range of s values. From eq 3.7 to 3.9, defining $\mathbf{H}'$ in region 1, and eq 3.21 and 3.22, defining $\mathbf{H}'$ in region 2, it can be seen that $\mathbf{Q}_1'$ and $\mathbf{Q}_2'$ have the following form in both of these extreme cases:

$$\mathbf{Q}_1' = F_1(R,a)(1 - 3\hat{R}\hat{R})\cdot(1 - \hat{u}_2\hat{u}_2) \quad (3.26)$$

and

$$\mathbf{Q}_2' = F_2(R,a)(1 - 3\hat{R}\hat{R})\cdot\hat{u}_2\hat{u}_2 \quad (3.27)$$

where we have used the fact that in region 1, $R = s$ and $\hat{R} = \hat{u}_1 = \hat{u}_2$. The functional forms of F_1 and F_2 in the two regions are, of course, different. Since eq 3.26 applies for extreme values of s, it is reasonable to assume that it will apply in the intermediate case as well. We determine x_1, x_2, z_1, and z_2 by requiring that $\langle\mathbf{H}'\rangle_{\hat{u}_1}$ be continuous at $s = b/2\lambda$, which means that

$$\mathbf{Q}_{1c}'\left(\frac{b}{2\lambda}\right) = \left\langle\mathbf{Q}_{1d}'\left(\frac{b}{2\lambda}\right)\right\rangle_{\hat{u}_1} \quad (3.28)$$

and

$$\mathbf{Q}_{2c}'\left(\frac{b}{2\lambda}\right) = \left\langle\mathbf{Q}_{2d}'\left(\frac{b}{2\lambda}\right)\right\rangle_{\hat{u}_1} \quad (3.29)$$

The persistence length of a polymer molecule is usually much larger than its cross-section radius, so we choose b and a to correspond to $b \gg 4\lambda a$ and use the expressions for $\mathbf{Q}_{1c}'$ and $\mathbf{Q}_{2c}'$ valid in the limit of $s \gg a$. These are obtained by taking derivatives with respect to s of $q_{1c}(s)$ and $q_{2c}(s)$, given by eq 3.17 and 3.18. Thus we have

$$\mathbf{Q}_{1c}' = (1 - \hat{u}_1\hat{u}_1)\left(\frac{a}{2s^3} - \frac{3a^3}{2s^5} + \dots\right) \quad (3.30)$$

and

$$\mathbf{Q}_{2c}' = \hat{u}_1\hat{u}_1\left(\frac{2}{s^3} - \frac{6a^2}{s^5} + ...\right) \tag{3.31}$$

x_1 and z_1 are then obtained by equating eq 3.24 to 3.30 at $s = b/2\lambda$, with the result

$$x_1 = \frac{25}{12}\left(\frac{\pi b^3}{3}\right)^{1/2}\left[1 - \frac{12(a\lambda)^2}{b^2}\right] - \frac{b^2}{4} + \frac{743b}{1260} \tag{3.32}$$

and

$$z_1 = \frac{1057}{504}b - \frac{11}{36}b^2 + x_1 \tag{3.33}$$

Similarly, x_2 and z_2 are obtained from eq 3.25 and 3.31 and are given by

$$x_2 = \left(\frac{221}{30b} - 1\right)\frac{b^2}{4} \tag{3.34}$$

and

$$z_2 = 25\left(\frac{\pi b^3}{3}\right)^{1/2}\left[1 - \frac{12(a\lambda)^2}{b^2}\right] - \left(\frac{5}{3} + \frac{3089}{70b}\right)\frac{b^2}{4} \tag{3.35}$$

If our model is reasonable, the results for G_a, ϵ, and the LS intensities will not be very sensitive to the choice of b. In section V we show that this is indeed the case for a wide range of b values and for reasonable values of the other parameters.

D. Expression for $\mathbf{G}_a$. From the results of subsections A, B, and C we can construct an approximate expression for $\langle\mathbf{H}(s_1)\rangle_{\hat{u}_1}$ valid for any s_1. As can be seen from eq 3.8, 3.9, 3.24, and 3.25, $\langle\mathbf{H}\rangle_{\hat{u}_1}$ always had the form

$$\langle\mathbf{H}(s_1)\rangle_{\hat{u}_1} = A(s_1)\mathbf{1} - B(s_1)\hat{u}_1\hat{u}_1 \tag{3.36}$$

where A and B are scalar functions of s_1. Using this expression, the scalar and second-rank parts of $\mathbf{G}_a$ can be written in terms of A and B as

$$\mathbf{G}_a(s_1) = G_a^{(0)}(s_1)\mathbf{1} + G_a^{(2)}(s_1)(\hat{u}_1\hat{u}_1 - \tfrac{1}{3}\mathbf{1}) \tag{3.37}$$

where

$$G_a^{(0)}(s_1) = \frac{1}{1 + A(s_1)} + \frac{1}{3}G_a^{(2)}(s_1) \tag{3.38}$$

and

$$G_a^{(2)}(s_1) = \frac{B(s_1)}{[1 + A(s_1)][1 + A(s_1) - B(s_1)]} \tag{3.39}$$

Contributions to A and B from the "cylinder" and "dipolar" regions vary according to the location of s_1 in the molecule and depend on the relative sizes of b and λL. Three cases may be distinguished:

Case 1. $b \geq 2\lambda L$

The field inside the molecule is given by the field inside a finite cylinder. Thus A is given by

$$A(s_1) = A_c(s_1) + A_c(L - s_1) \tag{3.40}$$

An equivalent expression holds for B, with B_c replacing A_c. A_c and B_c are derived in Appendix B by using the results of part A of this section.

Case 2. $\lambda L \leq b < 2\lambda L$

A and B have different functional forms for s_1 in three regions. A is given by the following:

region 2.1: $0 \leq s_1 < L - b/2\lambda$

$$A(s_1) = A_c(s_1) + A_c(b/2\lambda) + A_d(L - s_1) \tag{3.41a}$$

region 2.2: $L - b/2\lambda \leq s_1 < b/2\lambda$

$$A(s_1) = A_c(s_1) + A_c(L - s_1) \tag{3.41b}$$

and

region 2.3: $b/2\lambda \leq s_1 < L$

$$A(s_1) = A_c(L - s_1) + A_c(b/2\lambda) + A_d(s_1) \tag{3.41c}$$

Equivalent expressions hold for B, with B_c and B_d replacing A_c and A_d. A_d and B_d are derived by using the results of part B of this section and are explicitly given in Appendix B.

Case 3. $b < \lambda L$

This is the case of long polymer chains and is expected to correspond to the most common situation. A has different functional forms in the following three regions.

region 3.1: $0 \leq s_1 \leq b/2\lambda$

$$A(s_1) = A_c(s_1) + A_c(b/2\lambda) + A_d(L - s_1) \tag{3.42a}$$

region 3.2: $b/2\lambda < s_1 \leq L - b/2\lambda$

$$A(s_1) = 2A_c(b/2\lambda) + A_d(L - s_1) + A_d(s_1) \tag{3.42b}$$

and

region 3.3: $L - b/2\lambda < s_1 \leq L$

$$A(s_1) = A_c(b/2\lambda) + A_c(L - s_1) + A_d(s_1) \tag{3.42c}$$

Again B is obtained by replacing A_c and A_d with B_c and B_d in eq 3.42.

The expressions for A and B simplify considerably in the case of long chains. As L increases, region 3.3 disappears and the size of region 3.2 grows relative to that of region 3.1. As a result, in the limit $L \to \infty$, we have

$$\lim_{L\to\infty} A(s_1) = A_\infty = 2A_c(b/2\lambda) + 2A_d(\infty) \tag{3.43a}$$

and

$$\lim_{L\to\infty} B(s_1) = B_\infty = 2B_c(b/2\lambda) + 2B_d(\infty) \tag{3.43b}$$

A and B become independent of s_1. The above equations simplify still further in the case where the molecule is stiff as well as long, which means that λ becomes small. Equations 3.43 can then be expanded in powers of $a\lambda$, with the result

$$A_\infty \cong y_1/2 + \mathcal{O}[(a\lambda)^2] \tag{3.44a}$$

and

$$B_\infty \cong y_1/2 + \mathcal{O}[(a\lambda)^2] \tag{3.44b}$$

The leading terms are now those that would be present in an infinite cylinder. In this case A_∞ becomes equal to B_∞ and independent of y_2.

$$\lim_{\lambda\to 0} A_\infty = \lim_{\lambda\to 0} B_\infty = A_{\infty,c} = y_1/2 \tag{3.45}$$

The above expressions may also be obtained from eq 3.40, corresponding to case 1, in the limit of large L. As can be seen from eq 2.6a, y_1 depends only on the component of ϵ_p perpendicular to the molecular axis. In this limiting case $G_a^{(0)}$ and $G_a^{(2)}$ take on values well-known from classical electrodynamics,[8] namely

$$\lim_{\substack{L\to\infty \\ \lambda\to 0}} G_a^{(0)} = G_{ac}^{(0)} = \frac{6 + y_1}{3(2 + y_1)} = \frac{5\epsilon_s + \epsilon_{p\perp}}{3(\epsilon_s + \epsilon_{p\perp})} \tag{3.46}$$

and

$$\lim_{\substack{L\to\infty \\ \lambda\to 0}} G_a^{(2)} = G_{ac}^{(2)} = \frac{y_1}{2 + y_1} = \frac{\epsilon_{p\perp} - \epsilon_s}{\epsilon_{p\perp} + \epsilon_s} \quad (3.47)$$

These values are independent of the molecular size and shape. As can be seen from eq 3.43, if the molecule is long, but flexible, A, B, and the resulting $G_a^{(0)}$ and $G_a^{(2)}$ do not depend on L but still depend on the structural parameters a and λ.

Thus we have shown that the local field at a point s_1 inside a polymer molecule is, in general, dependent on the molecular size, conformation, and the distance of s_1 from the chain ends. In the next two sections we examine the consequences of this dependence on the refractive index and the intensity of scattered light of dilute polymer solutions.

IV. Dielectric Constant and Refractive Index Increment

In this section we present the results for ϵ and the refractive index increment, dn/dc, obtained with the expression for $\mathbf{G}_a$ derived in the previous section. Substituting eq 3.37 into eq 2.18, we get

$$\epsilon = \epsilon_s + cwD \quad (4.1)$$

and

$$\frac{dn}{dc} = \frac{w}{2\epsilon_s^{1/2}} D \quad (4.2)$$

where $w = \pi a^2 L$ is the volume of a polymer molecule and D is given by

$$D = \frac{1}{L}\int_0^L ds\, K_{iso}(s) \quad (4.3)$$

K_{iso} is the isotropic local field defined as

$$K_{iso}(s) = (\epsilon_p^0 - \epsilon_s) G_a^{(0)}(s) + \frac{2}{9}\Delta\epsilon_p G_a^{(2)}(s) \quad (4.4)$$

K_{iso} itself is in some cases only weakly dependent on the molecular size and shape. In particular, if the molecule is long, $G_a^{(0)}$ and $G_a^{(2)}$ are independent of s so that K_{iso} becomes equal to D. Using eq 3.43, we find

$$\lim_{L\to\infty} D = \lim_{L\to\infty} K_{iso} = K_{iso,\infty} = \frac{1}{1 + A_\infty}\left[(\epsilon_p^0 - \epsilon_s) + \frac{B_\infty(\epsilon_p^0 - \epsilon_s + \frac{2}{3}\Delta\epsilon_p)}{3(1 + A_\infty - B_\infty)}\right] \quad (4.5)$$

This value of K_{iso} is independent of L but does depend on λ and a. If the molecule is stiff as well as long, we may use eq 3.45, which becomes valid when $(a\lambda)^2 \ll 1$. If this limit K_{iso} becomes independent of molecular shape and dimensions

$$\lim_{a\lambda\to 0} K_{iso,\infty} = K_{iso,c} = \frac{(\epsilon_p^0 - \epsilon_s)(5\epsilon_s + \epsilon_p^0 + \Delta\epsilon_p/3) - \frac{2}{9}(\Delta\epsilon_p)^2}{3(\epsilon_p^0 + \epsilon_s - \Delta\epsilon_p/3)} \quad (4.6)$$

For many reasonable choices of the molecular dimensions and persistence length, eq 4.6 gives an accurate value of K_{iso} and of the resulting D. This quantity is then chiefly dependent upon solvent and solute dielectric tensor components. The dependence of ϵ and dn/dc on other molecular properties is mainly through w, so that these quantities are insensitive to molecular conformation but depend mainly on molecular size or the number of monomeric units. This result is not surprising in view of the fact that the Clausius–Mossotti equation,[9] which is independent of intermolecular correlations and of molecular conformation, describes accurately the dielectric constant of many liquid systems.

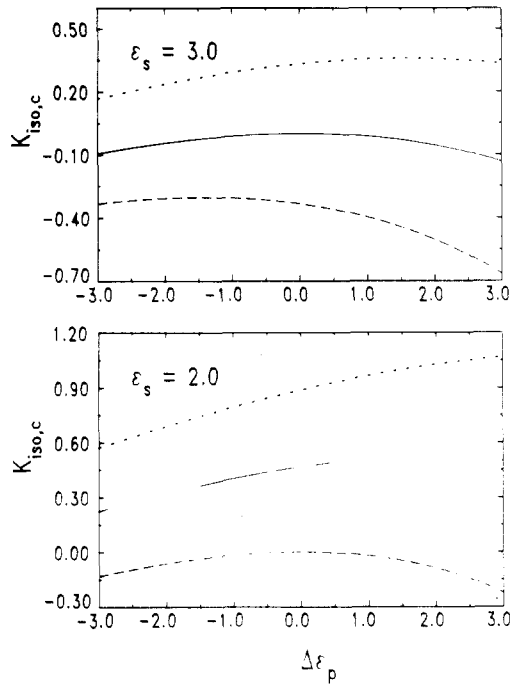

Figure 2. Dependence of the isotropic local field factor, K_{iso}, evaluated in the infinite cylinder approximation on polymer and solvent dielectric tensor components. Depicted is $K_{iso,c}$ as a function of $\Delta\epsilon_p$ for $\epsilon_p^0 = 2.0$ (dashed line), $\epsilon_p^0 = 3.0$ (full line), and $\epsilon_p^0 = 4.0$ (dotted line). The upper panel is for $\epsilon_s = 3.0$, the lower for $\epsilon_s = 2.0$.

Given that K_{iso} and D are well approximated by $K_{iso,c}$ in many cases, insights into the behavior of D as a function of ϵ_p^0 and $\Delta\epsilon_p$ may be gained by examining that of $K_{iso,c}$. The situation corresponding to $y_2 = 0$ was studied in I. In that case, D was shown to vanish when $\epsilon_p^0 = \epsilon_s$. In the present case, D would not vanish when $\epsilon_p^0 = \epsilon_s$ if $\Delta\epsilon_p \neq 0$ but would take on the value

$$D = \frac{2}{9L}\Delta\epsilon_p \int_0^L G_a^{(2)}(s)\, ds \quad (4.7)$$

where the value of $G_a^{(2)}$ appropriate for $y_1 = y_2/3$ is used. This quantity usually turns out to be negative as can be seen from the value of $K_{iso,c}$ for $y_1 = -y_2/3$

$$K_{iso,c} = -\frac{2}{9}\frac{(\Delta\epsilon_p)^2}{6\epsilon_s - \Delta\epsilon_p} \quad (4.8)$$

which is negative provided that $\Delta\epsilon_p < 6\,\epsilon_s$. This condition should always be satisfied by real systems at optical frequencies. The behavior of $K_{iso,c}$ as a function of $\Delta\epsilon_p$ for several values of ϵ_p^0 and ϵ_s is depicted in Figure 2. It can be seen from this figure that $K_{iso,c}$ depends more strongly on ϵ_p^0 than on $\Delta\epsilon_p$ but that the dependence on $\Delta\epsilon_p$ is by no means negligible. The figure shows that the presence of optical anisotropy in $\mathbf{D}_p$ may either enhance or decrease the isotropic local field and the resulting dn/dc relative to their values in the absence of $\Delta\epsilon_p$. As expected, $K_{iso,c}$ and the resulting dn/dc are negative when $\epsilon_p^0 \leq \epsilon_s$.

Experiments on dn/dc of polymers of different L in a given solvent show that this quantity is not always a linear function of L.[10] In some cases the sign of dn/dc changes as L is varied.[10] The approximation discussed above, $K_{iso} \cong K_{iso,c}$, gives rise to a linear relation between L and dn/dc, if the polymer dielectric tensor components are assumed

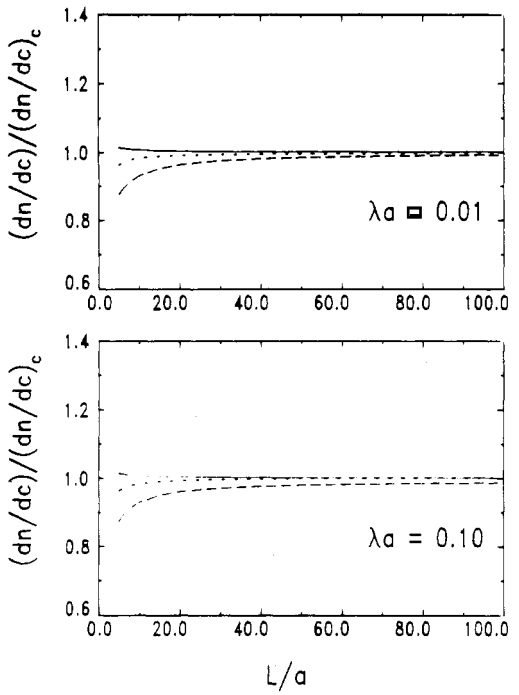

Figure 3. Influence of L and λ dependence of the local field on refractive index increment, dn/dc. Depicted is the ratio of dn/dc to $(dn/dc)_c$, its counterpart in the ICA, as a function of the reduced chain length, L/a. The upper panel is for $\lambda a = 0.01$, and the lower panel is for $\lambda a = 0.1$. Dashed line represents $\Delta\epsilon_p = 3.0$, full line $\Delta\epsilon_p = 0.0$, and dotted line $\Delta\epsilon_p = -3.0$. The other parameters are $\epsilon_p^0 = 4.0$, $\epsilon_s = 3.0$, and $b = 1.0$.

to be independent of L. A nonlinear relation for shorter chains is obtained if this approximation is not used. We examine now the L and λ dependence of D. This is done by comparing D to $K_{iso,c}$ or, equivalently, dn/dc to its counterpart calculated with the infinite cylinder approximation (ICA) to the field, which we denote by $(dn/dc)_c$. Figure 3 shows the results obtained. Overall, the figure shows that the ICA is a good approximation to the more accurate version of our model for dn/dc. The figure depicts $D/K_{iso,c}$ as a function of L/a for fixed values of ϵ_s and ϵ_p^0 and three values of $\Delta\epsilon_p$. The lower panel is for a flexible chain ($\lambda a = 0.1$), and the upper panel is for a relatively stiff chain ($\lambda a = 0.01$). Comparison of the upper and lower panels indicates that the ICA is more reasonable for stiff chains than for flexible chains, a result that agrees with our expectations. In the limit of very short chains ($L/a \leq 5$), the field for both values is given by the finite cylinder expression, eq 3.40, which is independent of λ. Thus the upper and lower panels give the same values of D in this range of chain lengths. It is also seen from both panels that the ICA becomes more accurate as L increases, which again is an expected result. Figure 3 shows that $D/K_{iso,c}$ deviates more strongly from unity when the magnitude of $\Delta\epsilon_p$ is increased. The reason for this is that when $\Delta\epsilon_p$ increases, the contribution of the anisotropic component of the local field, $G_a^{(2)}$, increases relative to that of the isotropic component, $G_a^{(0)}$. $G_a^{(2)}$ is more strongly dependent on the molecular size and shape than $G_a^{(0)}$ is. (This may be seen from eq 3.38 and 3.39, where the shape- and size-dependent terms A and B are quantities small in magnitude compared with unity, for the present choice of parameters. To lowest order in A and b, $G_a^{(0)} \sim 1$ and $G_a^{(2)} \sim B$.)

V. Light Scattering Intensity

In order to evaluate the isotropic and anisotropic (depolarized) LS intensities we need to choose a specific scattering geometry. We choose the incident field to be polarized along the z axis and the xy plane to be the scattering plane.[1a] This leads to

$$\hat{n}_i = \hat{k} \tag{5.1}$$

$$\mathbf{k}_i = k(\cos\alpha\hat{i} - \sin\alpha\hat{j}) \tag{5.2}$$

$$\mathbf{k}_f = k\hat{i} \tag{5.3}$$

and

$$\hat{n}_f = \hat{j} \quad \text{for VH scattering} \tag{5.4}$$

or

$$\hat{n}_f = \hat{k} \quad \text{for VV scattering} \tag{5.5}$$

where α is the scattering angle. The scattering wavevector, $\mathbf{q}$, is then

$$\mathbf{q} = \mathbf{k}_f - \mathbf{k}_i = q\hat{q} \tag{5.6}$$

where

$$q = 2k\left|\sin\frac{\alpha}{2}\right| \tag{5.7}$$

and

$$\hat{q} = \sin\frac{\alpha}{2}\hat{i} + \cos\frac{\alpha}{2}\hat{j} \tag{5.8}$$

Equation 2.20, defining the LS intensity, may be written as

$$I_{fi}(q) = \frac{k_0^4 cw^2}{[(4\pi)^2 r_0]^2}|\langle E\rangle|^2 M_{fi}(q) \tag{5.9}$$

The dependence of the LS intensity on the molecular conformation is contained in $M_{fi}(q)$. The persistence length measures the range intramolecular correlations. Consequently, the strength of the q dependence of M_{fi} is determined by the relative magnitudes of q and λ. In particular, if $(q/\lambda)^2 \ll 1$, as is the case for flexible chains or for low scattering angles, M_{fi} may be expanded in powers of q^2

$$M_{fi}(q) = \sum_{n=0}^{\infty}\frac{(-1)^n}{(2n)!}M_{fi}^{(2n)}q^{2n} \tag{5.10}$$

where

$$M_{fi}^{(2n)} = \frac{\partial^{(2n)}}{\partial q^{(2n)}}M_{fi}(q)|_{q=0} \tag{5.11}$$

We focus our attention on the two leading terms in this series. For VH, or anisotropic, scattering $M_{VH}^{(2n)}$ is given by

$$M_{VH}^{(2n)} = \frac{1}{L^2}\int_0^L ds_1 \int_0^L ds_2\, K_{VH}(s_1)K_{VH}(s_2)m_{VH}^{(2n)}(|s_1 - s_2|) \tag{5.12}$$

where

$$K_{VH}(s_i) = G_a^{(0)}(s_i)\Delta\epsilon_p + G_a^{(2)}(s_i)(\epsilon_p^0 - \epsilon_s + \tfrac{1}{3}\Delta\epsilon_p) \tag{5.13}$$

and for $n = 0$ and 1, $m_{VH}^{(2n)}$ are, respectively, given by

$$m_{VH}^{(0)}(s) = \langle(\hat{j}\cdot\hat{u}_1\hat{u}_1\cdot\hat{k})(\hat{j}\cdot\hat{u}_2\hat{u}_2\cdot\hat{k})\rangle \tag{5.14}$$

and

$$m_{VH}^{(2)}(s) = \langle(\hat{j}\cdot\hat{u}_1\hat{u}_1\cdot\hat{k})(\hat{j}\cdot\hat{u}_2\hat{u}_2\cdot\hat{k})(\hat{q}\cdot\mathbf{R}_{12})^2\rangle \tag{5.15}$$

Here we have used the approximation $r_{12} \cong R_{12}$, which is valid when $R_{12} \gg a$, a situation that occurs for most of the conformations corresponding to a large contour length,

$|s_1 - s_2|$. Conformations corresponding to a small value of R_{12} lead to a negligible value of $(\mathbf{q}\cdot\mathbf{r}_{12})^2$ and we are justified in ignoring their contribution to $M_{VH}^{(2)}$.

$M_{VV}(q)$ is given by

$$M_{VV}(q) = M_{iso}(q) + \tfrac{4}{3}M_{VH}(q) \tag{5.16}$$

where $M_{iso}(q)$ corresponds to the isotropic LS intensity and its leading terms $M_{iso}^{(0)}$ and $M_{iso}^{(2)}$ are

$$M_{iso}^{(0)} = \left[\frac{1}{L}\int_0^L ds\ K_{iso}(s)\right]^2 \tag{5.17}$$

and

$$M_{iso}^{(2)} = \frac{1}{L^2}\int_0^L ds_1 \int_0^L ds_2\ K_{iso}(s_1)K_{iso}(s_2)\langle(\hat{q}\cdot\mathbf{R}_{12})^2\rangle \tag{5.18}$$

with K_{iso} defined in eq 4.4. Comparing eq 5.17 and 4.2, we obtain the following well-known relation[11] between $I_{iso}(0)$ and dn/dc

$$\left(\frac{dn}{dc}\right)^2 = \frac{1}{c\epsilon_s}\left[\frac{8\pi^2 r_0}{k_0^2|\langle E\rangle|}\right]^2 I_{iso}(0) \tag{5.19}$$

The above equation is a consequence of the approximation $\mathbf{G} \cong \mathbf{G}_a$ made in section II. Had the contribution from $\Delta\mathbf{H}$ to $\mathbf{G}$ been retained, this relation between I_{iso} and dn/dc would no longer hold.

Using eq 3.2, we may express $\mathbf{R}_{12}$ in terms of a unit vector tangent to the molecular axis. Thus the averages in eq 5.14, 5.15, and 5.18 all involve just tangential unit vectors. They are evaluated by using the distribution function $g(\hat{u}_1,\hat{u}_2)$ for a pair of these vectors[1b]

$$g(\hat{u}_1,\hat{u}_2) = \frac{1}{(4\pi)^2}\sum_{l=0}^{\infty}(2l+1)\exp[-l(l+1)\lambda|s_1 - s_2|] \times \sum_{m=0}^{l} e_m \frac{(l-m)!}{(l+m)!}P_l^m(\cos\Theta_1)P_l^m(\cos\Theta_2)\cos[m(\Phi_1 - \Phi_2)] \tag{5.20}$$

where Θ_i and Φ_i are, respectively, the polar and azimuthal angles of $\hat{u}_i$ in the laboratory frame, P_l^m are associated Legendre functions, $e_0 = 1$, and $e_m = 2$ for $m \neq 0$. After averaging, eq 5.14 and 5.18 become

$$m_{VH}^{(0)}(s) = \tfrac{1}{15}e^{-6\lambda s} \tag{5.21}$$

and

$$M_{iso}^{(2)} = \frac{1}{3L^2\lambda}\int_0^L ds_1 \int_0^L ds_2\ K_{iso}(s_1)K_{iso}(s_2)\left[s + \frac{1}{2\lambda}(e^{-2\lambda s} - 1)\right] \tag{5.22}$$

The average in eq 5.15 involves four different tangent vectors and is somewhat more difficult to perform. The derivation is given in Appendix C and the result is

$$m_{VH}^{(2)}(s) = \frac{1}{105\lambda}\exp(-6\lambda s)\left\{\frac{1}{3}\left[s - \frac{1}{6\lambda}(1 - e^{-6\lambda s})\right] + \left[\frac{1}{30\lambda}e^{-6\lambda s} + \frac{7}{40\lambda}e^{4\lambda s} - \frac{s}{2} - \frac{5}{24\lambda}\right]\cos^2\frac{\alpha}{2}\right\} \tag{5.23}$$

In a general case the integrations over s_1 and s_2 in M_{VH} and M_{iso} have to be evaluated numerically. They can be done analytically in the case of long chains, since K_{VH} and K_{iso} become constant in the limit $\lambda L \gg 1$. These values of K_{VH} and K_{iso} are obtained by using eq 3.43 and are denoted by subscript "∞", which is also used to label the resulting M_{iso} and M_{VH} given by

$$M_{iso,\infty}^{(0)} = K_{iso,\infty}^2 \tag{5.24}$$

$$M_{iso,\infty}^{(2)} = \tfrac{2}{3}K_{iso,\infty}^2\langle S^2\rangle \tag{5.25}$$

$$M_{VH,\infty}^{(0)} = K_{VH,\infty}^2\frac{1}{45\lambda L}\left[1 + \frac{1}{6\lambda L}(e^{-6\lambda L} - 1)\right] \tag{5.26}$$

and

$$M_{VH,\infty}^{(2)} = K_{VH,\infty}^2\frac{1}{3780\lambda^4L^2}\left\{\frac{1}{3}\left[e^{-6\lambda L}\left(\frac{1}{3} + 2\lambda L\right) + \frac{e^{-12\lambda L}}{12} + \lambda L - \frac{5}{12}\right] + \cos^2\frac{\alpha}{2}\left[\frac{e^{-12\lambda L}}{60} + \frac{63}{20}e^{-2\lambda L} - e^{-6\lambda L}\left(\frac{3}{4} + \lambda L\right) + 3\lambda L - \frac{29}{12}\right]\right\} \tag{5.27}$$

$\langle S^2\rangle$ in eq 5.25 is the mean squared radius of gyration, which has the value[1b]

$$\langle S^2\rangle = L^2\left[\frac{1}{6\lambda L} - \frac{1}{4(\lambda L)^2} + \frac{1}{4(\lambda L)^3} - \frac{1}{8(\lambda L)^4}(1 - e^{-2\lambda L})\right] \tag{5.28}$$

$K_{iso,\infty}$ is given in eq 4.5 and $K_{VH,\infty}$ is

$$K_{VH,\infty} = \frac{1}{1 + A_\infty}\left[\Delta\epsilon_p + \frac{B_\infty(3\epsilon_p^0 - 3\epsilon_s + 2\Delta\epsilon_p)}{3(1 + A_\infty - B_\infty)}\right] \tag{5.29}$$

As can be seen from eq 5.25 and 5.28, $K_{iso,\infty}^2$ and $\langle S^2\rangle$ depend on the molecular conformation, so that for a long, flexible chain $M_{iso}^{(2)}$ is *not* simply related to $\langle S^2\rangle$ and will not, in general, be simply proportional to this quantity as is routinely assumed.[1a,b] Similarly, eq 5.26 and 5.27 differ from the corresponding expressions obtained with the bond additive or independent scatterer approximation.[12,13] Equations 5.24 to 5.27 take on the independent scatterer conformation dependence *only* when the chains are relatively rigid as well as long, i.e., in the limit $a\lambda \ll 1$, since $K_{VH,\infty}$ and $K_{iso,\infty}$ become independent of molecular conformation only in this case. These quantities are labeled by a subscript "c". $K_{iso,c}$ given by eq 4.6 and $K_{VH,c}$ by

$$K_{VH,c} = \frac{(\Delta\epsilon_p/3)(5\epsilon_s + \epsilon_p^0 - \tfrac{2}{3}\Delta\epsilon_p) + (\epsilon_p^0 - \epsilon_s)^2}{\epsilon_p^0 + \epsilon_s - \Delta\epsilon_p/3} \tag{5.30}$$

We may interpret $\pi a^2 K_{VH}$ as the effective anisotropic polarizability per unit chain length. It can be seen from eq 5.30 that the contributions from the shape anisotropy (proportional to $(\epsilon_p^0 - \epsilon_s)^2$) and the intrinsic anisotropy (proportional to $\Delta\epsilon_p$) are not simply additive. The assumption that these two contributions are additive is quite common in the literature,[14] even though its lack of validity was pointed out by Fortelny[15] several years ago.

Even the infinite cylinder approximation, which predicts conformation-independent isotropic and anisotropic local fields, represents an advance over the conventional independent scatterer approximation, since it contains the dependence of the LS intensities on the polymer dielectric tensor components. Some changes in this dependence are observed away from this limit, but the general trends stay the same, so it is instructive to study the behavior of the local field factors $K_{iso,c}$ and $K_{VH,c}$ as functions of ϵ_p^0, $\Delta\epsilon_p$, and ϵ_s. The behavior of $K_{iso,c}$ was discussed in section 4. Figure 4 depicts the behavior of $K_{VH,c}$ as a function of $\Delta\epsilon_p$ for several values of ϵ_p^0 and ϵ_s. It is seen that $K_{VH,c}$ is nearly a linear function of $\Delta\epsilon_p$. Its slope is positive and increases with increasing ϵ_p^0 at a fixed ϵ_s. The slope decreases as ϵ_s

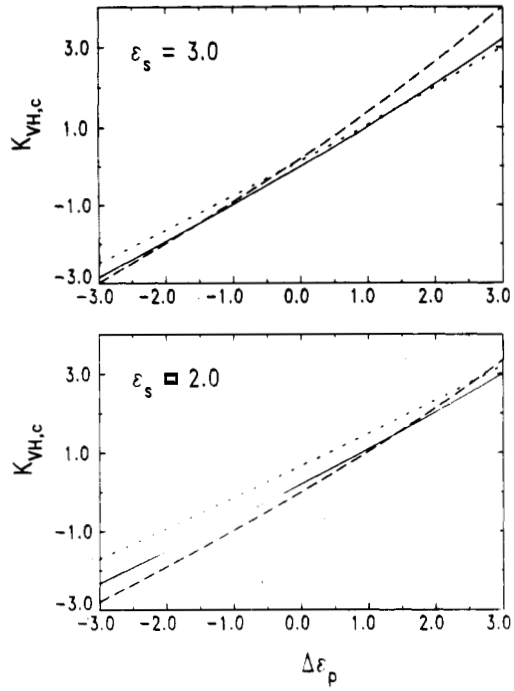

Figure 4. Dependence of the anisotropic local field factor, K_{VH}, evaluated in the ICA on polymer and solvent dielectric tensor components. Notation is the same as in Figure 2.

increases at a fixed ϵ_p^0. K_{VH} vanishes at $\Delta\epsilon_p = {}^3/_4(5\epsilon_s + \epsilon_p^0) - {}^3/_4[(5\epsilon_s + \epsilon_p^0)^2 + 8(\epsilon_p^0 - \epsilon_s)^2]^{1/2}$. This corresponds to $\Delta\epsilon_p = 0$ when $\epsilon_p^0 = \epsilon_s$ and to a small negative value of $\Delta\epsilon_p$ otherwise. In the absence of $\Delta\epsilon_p$, the "shape" anisotropy part of $K_{VH,c}$ would always be positive, so this can be thought of as a cancellation of "intrinsic" and "shape" optical anisotropies, even though these two contributions to $K_{VH,c}$ are not strictly additive. Given that $M_{VH,c}$ is proportional to $K_{VH,c}^2$, it is apparent from this figure that the depolarized intensity will increase when the magnitude of $\Delta\epsilon_p$ becomes large. Comparing Figures 2 and 4, we note that $K_{VH,c}$ depends more strongly on $\Delta\epsilon_p$ and less strongly on ϵ_p^0 than $K_{iso,c}$ does.

Given that the results for the L and λ dependence of LS intensities in the independent scatterer approximation are well-known and widely used, we focus our attention on the deviations from this behavior exhibited by our more realistic model. We examine the behavior of M_{iso}, M_{VH}, and the depolarization ratio for excess LS by polymers in solution, ρ, defined by

$$\rho = \frac{I_{VH}}{I_{iso}} = \frac{M_{VH}}{M_{iso}} \simeq \rho^{(0)} + \frac{q^2}{2}\rho^{(2)} \tag{5.31}$$

where

$$\rho^{(0)} = M_{VH}^{(0)}/M_{iso}^{(0)} \tag{5.32}$$

and

$$\rho^{(2)} = (M_{VH}^{(0)}M_{iso}^{(2)} - M_{iso}^{(0)}M_{VH}^{(2)})/(M_{iso}^{(0)})^2 \tag{5.33}$$

and compare them to the corresponding quantities obtained in the ICA. The results of this comparison, for molecular parameters the same as those used in Figure 3, are depicted in Figures 5–9. Before discussing in detail each of these figures, we point out their common features. At the chain lengths $L/a \leq 5.0$, the local fields are given by the finite cylinder expression, eq 3.40, which is independent of λ, so that the values of $M_{iso}^{(0)}$ are identical for both values of λa. The values of the other quantities are nearly identical in this range of L/a values as well. The deviations of all the quantities depicted from their ICA

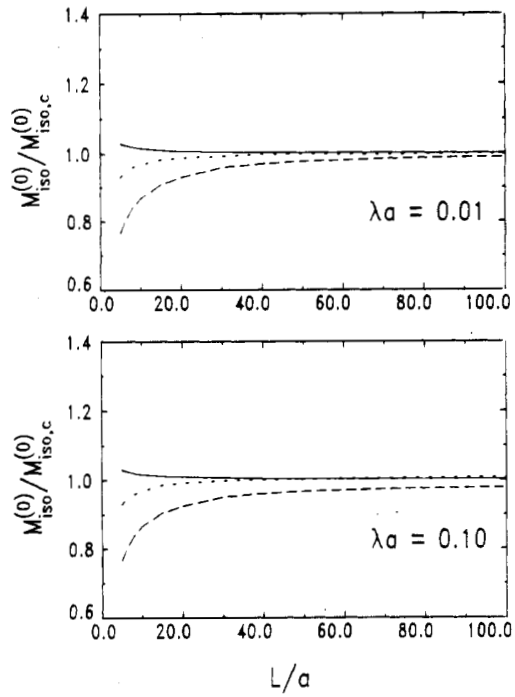

Figure 5. Influence of L and λ dependence of the local field on the $q = 0.0$ term in the isotropic LS intensity. Depicted is the ratio of $M_{iso}^{(0)}$ to $M_{iso,c}^{(0)}$, its counterpart in the ICA, as a function of the reduced chain length, L/a. Notation and values of other parameters are the same as in Figure 3.

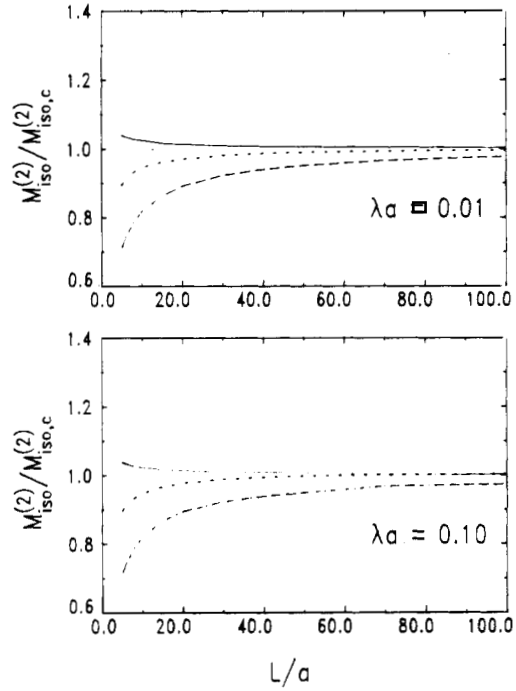

Figure 6. Influence of L and λ dependence of the local field on the term proportional to q^2 in the isotropic LS intensity. Depicted is the ratio of $M_{iso}^{(2)}$ to $M_{iso,c}^{(2)}$, its counterpart in the ICA, as a function of the reduced chain length, L/a. Notation and values of other parameters are the same as in Figure 3.

counterparts are more pronounced for more flexible chains and at shorter chain lengths. This result agrees with our expectations. In the case of short chains, the end effects on the local field are important. When the chains are relatively flexible, the persistence length dependence of the local field becomes nonnegligible. Consistent with the approximation $\mathbf{G} \simeq \mathbf{G}_a$, introduced in section 2, we find that all the quantities considered depend more strongly on L than on λ. It is important to realize that this ap-

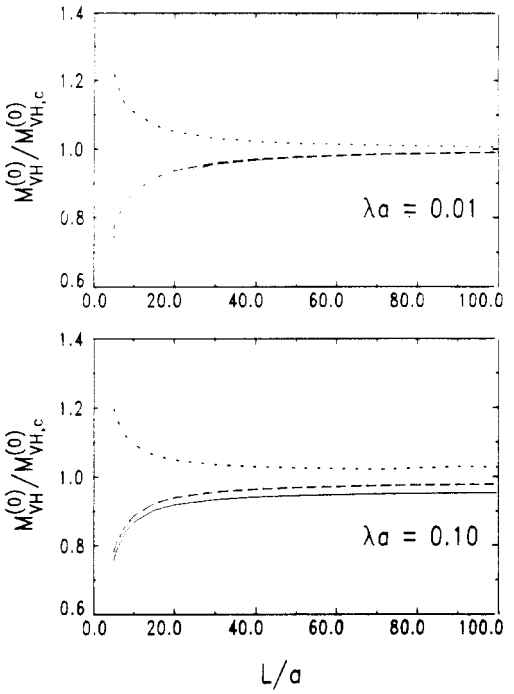

Figure 7. Influence of L and λ dependence of the local field on the $q = 0.0$ term in the depolarized LS intensity. Depicted is the ratio of $M_{VH}^{(0)}$ to $M_{VH,c}^{(3)}$, its counterpart in the ICA, as a function of the reduced chain length, L/a. Notation and values of other parameters are the same as in Figure 3.

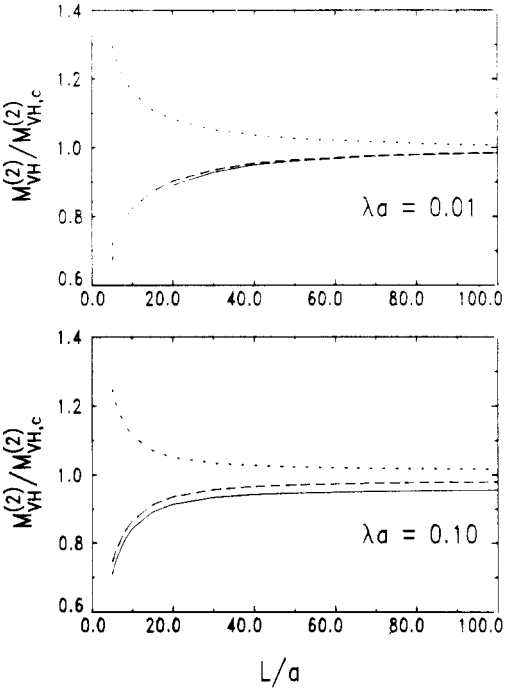

Figure 8. Influence of L and λ dependence of the local field on the term proportional to q^2 in the depolarized LS intensity. Depicted is the ratio of $M_{VH}^{(2)}$ to $M_{VH,c}^{(2)}$, its counterpart in the ICA, as a function of the reduced chain length, L/a. The scattering angle $\alpha = 30°$. Notation and values of other parameters are the same as in Figure 3.

proximation becomes less accurate for flexible chains, where the effects of the chain flexibility on the LS intensities are likely to be underestimated by our model.

We first consider in detail the isotropic LS intensity. Figures 5 and 6 depict, respectively, the ratios $M_{iso}^{(0)}/M_{iso,c}^{(0)}$ and $M_{iso}^{(2)}/M_{iso,c}^{(2)}$ as functions of L/a. The lower panels are for flexible chains, $\lambda a = 0.10$, and the upper panels are for stiff chains, $\lambda a = 0.01$. The dependence of

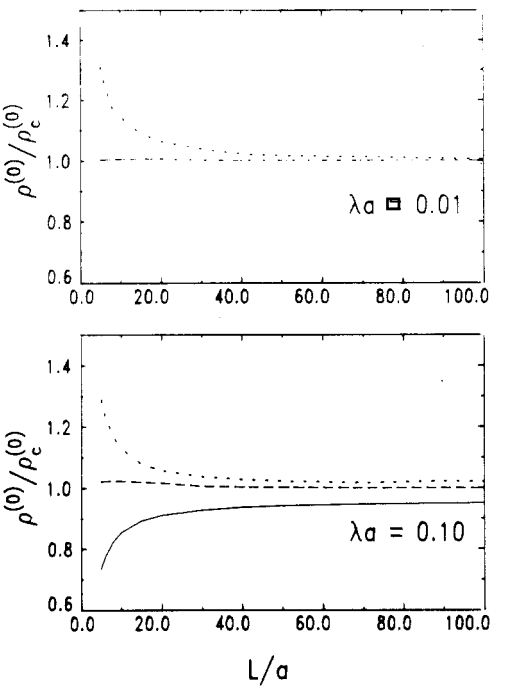

Figure 9. Influence of L and λ dependence of the local field on the $q = 0.0$ term in the depolarization ratio. Depicted is the ratio of $\rho^{(0)}$ to $\rho_c^{(0)}$, its counterpart in the ICA, as a function of the reduced chain length, L/a. Notation and values of other parameters are the same as in Figure 3.

$M_{iso}^{(2)}$ on $\Delta\epsilon_p$ is similar to that of $M_{iso}^{(0)}$, given that both of these quantities involve integrals over the chain length of the same local field factor, $K_{iso}(s_1)K_{iso}(s_2)$. The most pronounced deviations from ICA are seen for $\Delta\epsilon_p = 3.0$, and the smallest for $\Delta\epsilon_p = 0$. Negative deviations are observed in the former two cases, and positive deviations in the latter one. As discussed already in connection with Figure 3, the opposite trends are due to the absence of the contribution to K_{iso} from $G_a^{(2)}$ when $\Delta\epsilon_p = 0$. For all values of $\Delta\epsilon_p$, $M_{iso}^{(2)}$ shows somewhat larger deviations from the ICA than $M_{iso}^{(0)}$ does. In the ICA $M_{iso}^{(2)}$ is proportional to the mean squared radius of gyration, $\langle S^2 \rangle$. Figure 6 shows that this proportionality no longer holds in our model. The estimates of $\langle S^2 \rangle$ from LS measurements become less accurate as the chain length decreases, and its flexibility and local optical anisotropy increase. We note, however, that LS measurements of $\langle S^2 \rangle$ are possible only for relatively long chains, for which we predict relatively small deviations from the ICA for all cases depicted in Figure 6.

We consider next the depolarized intensity. The ratios $M_{VH}^{(0)}/M_{VH,c}^{(0)}$ and $M_{VH}^{(2)}/M_{VH,c}^{(2)}$ (at $\alpha = 30°$) as functions of L/a are depicted, respectively, in Figures 7 and 8. The appearance of the two figures is quite similar, given that they both involve integrals over the chain length of the same local field factors, $K_{VH}(s_1)K_{VH}(s_2)$. The deviations from the ICA are seen to be slightly more pronounced in the case of $M_{VH}^{(2)}$. Both figures illustrate that substantial deviations of the depolarized intensity from its value in the ICA occur for all three values of $\Delta\epsilon_p$ considered. The value of λ^{12} or, equivalently the energy difference between torsional local minima,[16] is frequently deduced from the intensity of low-angle depolarized LS, namely from $M_{VH}^{(0)}$ measured as a function of the chain length, L. To our knowledge, it has always been assumed in the data analysis that the local field factor K_{VH} is independent of L and λ, which leads to the L and λ dependence of $M_{VH}^{(0)}$ predicted by the ICA. We see from Figure 7 that this assumption would lead to serious errors in the values of torsional po-

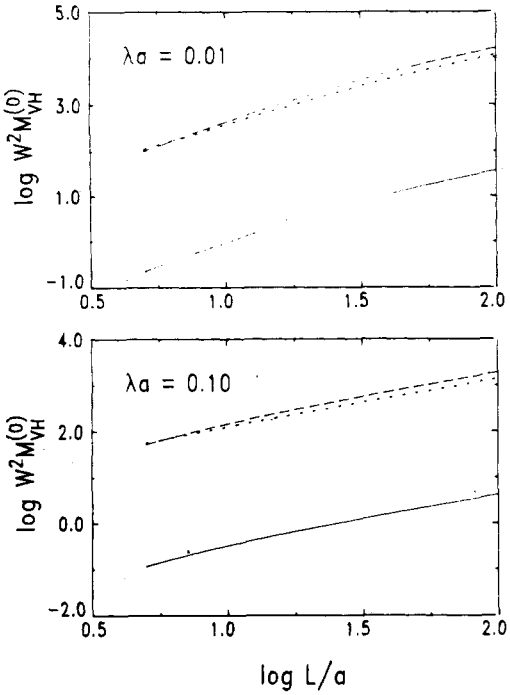

Figure 10. Logarithmic plot of depolarized LS intensity, evaluated at $q = 0.0$, as a function of the reduced chain length, L/a. Notation and values of other parameters are the same as in Figure 3.

tential parameters, especially in the case of short chains, where the differences between the values of $M_{VH}^{(0)}$ and $M_{VH,c}^{(0)}$ are large. For the values of $\Delta\epsilon_p$ depicted on this figure, use of the ICA would lead to an overestimate of λ for $\Delta\epsilon_p = -3.0$ and to an underestimate of λ for $\Delta\epsilon_p = 0$ and $\Delta\epsilon_p = 3.0$. Note that for $\Delta\epsilon_p = 0$ and $\Delta\epsilon_p = -3.0$, the deviations from the ICA exhibited by $M_{VH}^{(0)}$ are in the opposite direction from those exhibited by $M_{iso}^{(2)}$. There would thus be a large discrepancy between the values of λ estimated from isotropic and depolarized LS measurements. A comparison of the values of λ obtained from these measurements could thus be used to investigate the effects of the dependence of the local field on the chain dimensions. Note, however, that a consistency in the values of λ obtained would not mean that the ICA is valid, just that the isotropic and anisotropic local field factors deviate from it in the same direction. The results shown for $\Delta\epsilon_p = 3.0$ are an example of this. Figure 9 shows a comparison between the low-angle depolarization ratio, $\rho^{(0)}$, and its ICA counterpart, $\rho_c^{(0)}$ as functions of the chain length. The results for this quantity follow from the ones shown in Figures 5 and 7. We see that for $\Delta\epsilon_p = 3.0$, the differences from the ICA exhibited by $M_{VH}^{(0)}$ nearly cancel those shown by $M_{iso}^{(0)}$. Partial cancellation occurs for $\Delta\epsilon_p = 0$ and an enhancement is observed for $\Delta\epsilon_p = -3.0$. This figure demonstrates the chain length dependence of the local field may have an important effect on $\rho^{(0)}$.

Figure 10 depicts the depolarized low-angle LS intensity per molecule vs. the chain length, plotted on a logarithmic scale. This figure demonstrates that anisotropy in the polymer optical dielectric constant results in a large enhancement of the depolarized LS intensity. In I it was noted that, for most polymer molecules in solution, the refractive index increment data and the depolarized LS intensity cannot simultaneously be fit if the polymer dielectric tensor is assumed to be isotropic. A reasonable value of dn/dc may be obtained, but a value of I_{VH} too small by 1 or 2 orders of magnitude results. Here we see that $\Delta\epsilon_p$ of ± 3 results in an enhancement in $M_{VH}^{(0)}$ by a factor of about 350 over the value of $M_{VH}^{(0)}$ for $\Delta\epsilon_p = 0$.

Table I
Effect of Choice of b on Light Scattering Intensities[a]

b	λa	$M_{VH}^{(0)}$	$M_{VH}^{(2)}/a^2$	$M_{iso}^{(0)}$	$M_{iso}^{(2)}/a^2$
0.08		0.265	19.9	0.968	1.09×10^2
0.1		0.266	19.9	0.972	1.09×10^2
1.0	0.01	0.267	20.0	0.976	1.10×10^2
2.0		0.267	20.0	0.976	1.10×10^2
0.8		3.72×10^{-2}	0.122	0.960	39.5
1.0		3.74×10^{-2}	0.123	0.968	39.7
2.0	0.1	3.77×10^{-2}	0.124	0.976	40.0
4.0		3.78×10^{-2}	0.124	0.976	40.0

[a] Values of other parameters: $L/a = 50.0$, $\epsilon_p^0 = 4.0$, $\Delta\epsilon_p = 3.0$, and $\epsilon_s = 3.0$.

We have not yet carried out extensive comparisons between our model and experiments. Preliminary comparisons have been made with the $\rho^{(0)}$ data of Arpin et al.[12] for a dilute solution of poly(*p*-phenylene terephthalamide) in 96% sulfuric acid ($\epsilon_s = 2.045$). These data, as well as the results for dn/dc for this system, may be fit with a reasonable set of parameters, namely $a = 2.56$ Å (hydrodynamic radius of benzene[17]), $\epsilon_p^0 = 3.82$, and $\Delta\epsilon_p = 1.59$. Details of comparison of the model with these and other experimental results will be given in a future publication.[18]

The quantities depicted in Figures 3 and 5–10 have been evaluated by using $b = 1.0$. Table I shows the dependence of calculated isotropic and depolarized LS intensities on the choice of b for $L/a = 50$ and $\Delta\epsilon_p = 3.0$. b, defined by eq 3.28 and 3.29, determines the sizes of the "cylinder" and "dipolar" regions within the molecule. As can be seen from Figures 5–8, the ICA overestimates all the quantities listed in Table I for this choice of $\Delta\epsilon_p$. Thus an increase in b leads to an increase in these quantities, as long as $2\lambda L > b$. If $2\lambda L < b$, the intensities are independent of b. This situation is represented in the table by $\lambda a = 0.01$ with $b = 1$ and $b = 2$. It can be seen from the table that the results are only weakly dependent on the choice of b, for values of b of order of unity.

Figures 5–10 depict the behavior of LS intensities for three values of $\Delta\epsilon_p$ and for fixed values of ϵ_p^0 and ϵ_s. Analogous studies can be carried out by varying ϵ_p^0 at fixed $\Delta\epsilon_p$ and ϵ_s or by varying the solvent optical dielectric constant and keeping the polymer dielectric tensor components fixed. The latter study yields solvent effects on LS intensities. We have carried out such a study for two values of the chain length ($L/a = 10$ and $L/a = 50$) and for the other parameters representative of flexible polymers in organic solvents. The results of this study for isotropic and depolarized LS intensities as functions of ϵ_s are depicted in Figure 11. Only the $q = 0.0$ components of the intensities are represented, since the higher order terms are negligible for the present choices of L/a and λa. The figure depicts the ratios of the model intensities to those computed with the ICA. As expected, larger deviations from unity and stronger dependence on ϵ_s are exhibited by the ratios for the shorter of the two chains. $\Delta\epsilon_p$ is positive, which means that the intrinsic and the shape anisotropies enhance each other. As a result, the depolarized intensities are nonvanishing. Also the anisotropic local fields for finite, flexible chains are smaller than those for infinite rigid molecules. The isotropic intensity, which depends strongly on $\epsilon_p^0 - \epsilon_s$, vanishes in the range of ϵ_s depicted both in the ICA and in the finite chain local field model, in the vicinity of $\epsilon_p^0 = \epsilon_s$. The ratios depicted become infinite when $M_{iso,c}^{(0)}$ vanishes (at $\epsilon_s = 2.468$, for the present choice of ϵ_p^0 and $\Delta\epsilon_p$). Figure 11 shows that we would expect to observe different deviations from ICA to occur in different solvents for a polymer of given L and

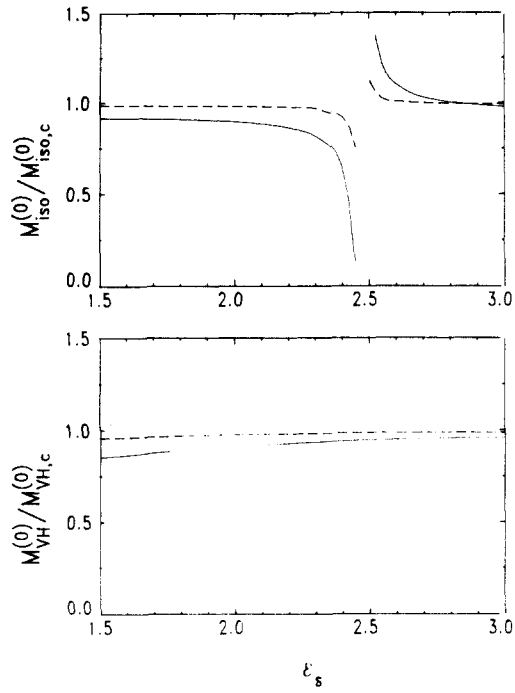

Figure 11. Dependence of isotropic (upper panel) and depolarized (lower panel) LS intensities, evaluated in the $q = 0.0$ limit, on the solvent optical dielectric constant ϵ_s. Depicted are ratios $M_{iso}^{(0)}/M_{iso,c}^{(0)}$ and $M_{VH}^{(0)}/M_{VH,c}^{(0)}$ for $L/a = 10$ (full line) and $L/a = 50$ (dashed line). The values of the other parameters are $\epsilon_p^0 = 2.5$, $\Delta\epsilon_p = 1.5$, $\lambda a = 0.10$, and $b = 1.0$.

λ. The use of ICA in interpreting LS data to obtain, e.g., λ in different solvents, for a known value of L would then lead to mistaking local field changes for structural changes.

VI. Concluding Remarks

We presented the results for the refractive index increment and the LS intensities calculated using continuum models for the polymer conformation and optical response. We summarize here our most important findings:

(a) We found that the local field at a point within a chain molecule depends on the molecular shape, size, and the distance of the point from the chain ends. The dependence on these parameters disappears only in the infinite cylinder approximation (ICA). The independent scatterer or bond additive approximation is equivalent to this approximation in its prediction of chain length and conformation dependence of LS intensities and refractive index increment. The dependence of the local field on chain dimensions is strongest for relatively short chains. The deviations of the LS intensities for solutions of these molecules from the ICA may be quite large, those of dn/dc somewhat smaller. The mean squared radius of gyration, $\langle S^2 \rangle$, is only approximately related to the quadratic term in the scattering wavevector in the isotropic LS intensity. The approximation is quite good for long chains for which LS can be used to measure $\langle S^2 \rangle$.

(b) We derived the dependence of the local field on the polymer dielectric tensor components, ϵ_p^0 and $\Delta\epsilon_p$, and on the solvent optical dielectric constant, ϵ_s. We showed that the polymer optical anisotropy is not simply a sum of intrinsic and shape anisotropy contributions, as is frequently assumed. We found that a different chain length and shape dependence of LS intensities and of dn/dc is obtained for different choices of values of $\Delta\epsilon_p$, ϵ_p^0, and ϵ_s. We also found that the inclusion of the intrinsic anisotropy into the model is essential in predicting the correct order of magnitude for depolarized LS intensities in most polymer solutions.

Our theory suggests several experiments to test the importance of local field effects on light scattering from polymer solutions. To investigate the breakdown of the ICA or of the independent scatterer approximation, one could measure $M_{VH}^{(0)}$, $\rho^{(0)}$, and $M_{iso}^{(2)}$ for a series of chain molecules containing different numbers of monomeric units and use the ICA to extract the values of λ from these experiments. Differences in the values of the persistence length obtained in different experiments would indicate deviations from the ICA. The strong dependence of LS intensities on ϵ_s, predicted by the theory, could be investigated by carrying out experiments in different solvents and deducing the chain persistence lengths from non-light scattering measurements.

It would be desirable to extend the range of validity of our model by removing some of the approximations used herein. In particular, the treatment of optical response of flexible chains would be improved by including, at least to first order, the fluctuations in the local field, which have been neglected in the present treatment (cf eq 2.26). We anticipate that inclusion of these fluctuations would lead to a prediction of larger deviations of LS intensities of long flexible chains from those predicted by the ICA. Another important improvement would result from a more accurate treatment of the contribution to the local field from a more accurate treatment of the contribution to the local field from the range of distances of the order of magnitude of the persistence length. This would be accomplished by extending the distribution function $f(\mathbf{R},\hat{u}_1,\hat{u}_2,s)$ into this range. Work on both of these problems is presently under way.

Acknowledgment. This work was supported in part by the National Science Foundation through Grant No. CHE-8007472. Computational work was supported in part by NIH Grant GM-27945.

Appendix A. Behavior of q_{1c} and q_{2c} near $s' = 0$

In this appendix we derive the values of q_{1c} and q_{2c} at $s' = 0$ and expressions for $T(1,s')$ and $T(-1,s')$. We first focus our attention on q_{1c}. Equation 3.13 indicates that $F(\rho_1,s')$ vanishes as $s' \to 0$ if $\rho_1 \neq a$. We thus examine the behavior of F as ρ_1 approaches the interior surface of the molecule; i.e., we consider $F(\rho_1,s')$ when $\rho_1 = a(1-\delta)$ in the limit $\delta \to 0$.

$$\lim_{\delta \to 0} F(a(1-\delta),s') = \frac{s'}{[4a^2 + s'^2]^{1/2}}\left[K\left(\frac{2a}{[4a^2 + s'^2]^{1/2}}\right) + \frac{\delta}{2}\Pi\left(\frac{\pi}{2},-\frac{4(1-\delta)}{(2-\delta)^2},\frac{2a}{[4a^2 + s'^2]^{1/2}}\right)\right] \quad \text{(A.1)}$$

When we take the limit $s' \to 0$, $s'K$ vanishes. Using the explicit expression for Π, we get

$$\lim_{\substack{\delta \to 0 \\ s' \to 0}} F(a(1-\delta),s') = \frac{s'}{[4a^2 + s'^2]^{1/2}}\frac{\delta}{2}\int_0^{\pi/2} d\alpha \frac{1}{\left[\frac{\delta^2}{4} + \cos^2\alpha\right]\left[1 - \frac{4a^2}{4a^2 + s'^2}\sin^2\alpha\right]^{1/2}} \quad \text{(A.2)}$$

It can be seen from this expression that the integrand becomes singular at $\alpha = \pi/2$ and is well-behaved away from this limit. In order to integrate over this singularity, we let $\theta = \alpha - \pi/2$ and expand around $\theta = 0$. The range

of integration is extended to ∞, since the significant contribution to the integral is from the region around the origin

$$\lim_{\substack{\delta\to 0\\ s'\to 0}} F(a(1-\delta),s') = s'\int_0^{\pi/2} \frac{\delta/2\, d\theta}{[\delta^2/4 + \sin^2\theta][4a^2 + s'^2 - 4a^2\cos^2\theta]^{1/2}} = \int_0^{\infty} \frac{\delta/2\, d\theta}{\delta^2/4 + \theta^2} \quad (A.3)$$

Integration over θ gives

$$\lim_{\substack{\delta\to 0\\ s'\to 0}} F(a(1-\delta),s') = \pi/2 \quad (A.4)$$

and integration over ρ_1 leads to eq 3.19. In I, this integration was not carried out. We used the approximation $q_{1c}(s') \cong (1/2\pi a)\lim_{\delta\to 0} F(a(1-\delta),s')$, which gives $q_{1c}(0) \cong 1/4a$. We found that the difference between the approximate q_{1c} used in I and the exact one used herein becomes negligible for values of $s' \geq a$.

In order to investigate the properties of q_{2c} near $s' = 0$, we first discuss the behavior of $T(\cos\phi,s')$ near $\phi = 0$ and $\phi = \pi$, where eq 3.16 appears to be singular. Even though this limiting behavior could be obtained by expanding eq 3.16 around $c = \pm 1$, it is simpler and more instructive to start with the following expression for $T(\cos\phi,s)$:

$$T(\cos\phi,s) = -s\int_0^a \rho_1\, d\rho_1 \int_0^a \rho_2\, d\rho_2 \frac{1}{r_{12}^3} \quad (A.5)$$

When $\phi = \pi$, r_{12} reduces to

$$r_{12} = [s^2 + (\rho_1 + \rho_2)^2]^{1/2} \quad (A.6)$$

The integrations over ρ_1 and ρ_2 are carried out with the result

$$T(-1,s) = \frac{1}{3s}(s^2+4a^2)^{3/2} - \frac{2}{3s}(s^2+a^2)^{3/2} + \frac{s^2}{3} - \frac{a^2}{s}[s^2+4a^2]^{1/2} \quad (A.7)$$

This expression vanishes in the limit $s \to 0$.

$$\lim_{s\to 0} T(-1,s) = \frac{8a^3}{3s} - \frac{2a^3}{3s} - \frac{2a^3}{s} = 0 \quad (A.8)$$

This result is not surprising since $\phi = \pi$ corresponds to ρ_1 and ρ_2 pointing in opposite directions, so it leads to $r_{12} = 0$ only when $\rho_1 = \rho_2$ and $s = 0$. We now consider the case $\phi = 0$, which corresponds to ρ_1 parallel to ρ_2. Now r_{12} becomes

$$r_{12} = [s^2 + (\rho_1 - \rho_2)^2]^{1/2} \quad (A.9)$$

and integration over ρ_1 and ρ_2 of eq A.5 results in

$$T(1,s) = \frac{2s^2}{3} - \frac{2(s^2+a^2)^{3/2}}{3s} + a^2 \quad (A.10)$$

This expression is well-behaved at finite s but becomes singular as s approaches 0

$$\lim_{s\to 0} T(1,s) = -\frac{2a^3}{3s} \to -\infty \quad (A.11)$$

This singularity in T is integrable, as will be shown below. To do this we expand $T(\cos\phi,s)$ for small ϕ and obtain the following expression:

$$\lim_{\phi\to 0} T(\cos\phi,s) = \frac{s}{\phi^2}[2s - 2[a^2+s^2]^{1/2}] + \frac{s^2}{\phi^3}\left\{\arctan\left(\frac{[s^2+a^2\phi^2]^{1/2}}{s\phi}\right) - \arctan\left(\frac{s}{\phi[a^2+s^2]^{1/2}}\right) + \arctan\left(\frac{\phi[a^2+s^2]^{1/2}}{s}\right)\right\} \quad (A.12)$$

Taking now the limit $s \to 0$, this expression becomes

$$\lim_{\substack{\phi\to 0\\ s\to 0}} T(\cos\phi,s) = \frac{a^3}{s}\left\{-\frac{2}{y^2} + \frac{1}{y^3}\left[\frac{\pi}{2} - \arctan\frac{1}{y} + \arctan y\right]\right\} \quad (A.13)$$

where $y = \phi a/s$. $q_{2c}(0)$ is obtained by integrating the above expression over y

$$q_{2c}(0) = \frac{4}{\pi a^2}\int_0^{\infty} dy \left[-\frac{2}{y^2} + \frac{1}{y^3}\left(\frac{\pi}{2} - \arctan\frac{1}{y} + \arctan y\right)\right] = \frac{4}{\pi a^2}[A(\infty) - A(0)] \quad (A.14)$$

where $A(y)$ is given by

$$A(y) = \frac{2}{y} - \frac{\pi}{4y^2} + \frac{1}{2y^2}\,\mathrm{arccot}\, y - \frac{1}{2y} - \frac{1}{2}\arctan y - \frac{1}{2}\left(\frac{1}{y^2}+1\right)\arctan y - \frac{1}{2y} \quad (A.15)$$

At the upper limit of integration A becomes

$$A(\infty) = -\pi/2 \quad (A.16)$$

Its value at $y = 0$ is obtained by expanding arccot y and arctan y for small y

$$\mathrm{arccot}\, y = \frac{\pi}{2} - y + \frac{y^3}{3} + \ldots \quad (A.17)$$

$$\arctan y = y - \frac{y^3}{3} + \frac{y^5}{5} - \ldots \quad (A.18)$$

Substitution of eq A.17 and A.18 into eq A.15 gives

$$A(0) = 0 \quad (A.19)$$

and substitution of the above equation and eq A.16 into eq A.14 leads to eq 3.20, the desired result.

Appendix B. Derivation of A_c, B_c, A_d, and B_d

Here we present explicit expressions for A_c, B_c, A_d, and B_d used in eq 3.40 to 3.42. We obtain A_c and B_c by integrating $\mathbf{H}_c'$, defined in eq 3.7, over s and using eq 3.12 and 3.15, with the result

$$\int_0^{s'} ds\, \mathbf{H}_c'(s) = y_1\frac{a}{2}(\mathbf{1} - \hat{u}_1\hat{u}_1)q_{1c}(s') - y_2\frac{a^2}{4}q_{2c}(s')\hat{u}_1\hat{u}_1 \quad (B.1)$$

$$= A_c(s')\mathbf{1} - B_c(s')\hat{u}_1\hat{u}_1 \quad (B.2)$$

Comparing eq B.1 to eq B.2, we find

$$A_c(s') = y_1\frac{a}{2}q_{1c}(s') \quad (B.3)$$

and

$$B_c(s') = y_1\frac{a}{2}q_{1c}(s') + y_2\frac{a^2}{4}q_{2c}(s') \quad (B.4)$$

Similarly, we define A_d and B_d by

$$\int_{b/2\lambda}^{s'} ds\ \langle \mathbf{H}_d'(s)\rangle_{\hat{u}_1} = \int_{b/2\lambda}^{s} ds\ [\langle \mathbf{Q}_{1d}'(s)\rangle_{\hat{u}_1} + \langle \mathbf{Q}_{2d}'(s)\rangle_{\hat{u}_1}] \tag{B.5}$$

$$= A_d(s')\mathbf{1} - B_d(s')\hat{u}_1\hat{u}_1 \tag{B.6}$$

The explicit expressions for A_d and B_d are obtained then by integrating eq 3.24 and 3.25 from $b/2\lambda$ to s'. They are

$$A_d(s') = \left(\frac{a\lambda}{5}\right)^2\left(\frac{12}{\pi b^3}\right)^{1/2}\left[y_1\left(1 - \frac{743}{525b} + \frac{12x_1}{7b^2}\right) - y_2\left(\frac{1}{6} - \frac{221}{300b} + \frac{2x^2}{7b^2}\right)\right] - \left(\frac{a\lambda}{5}\right)^2\left(\frac{3}{2\pi t^3}\right)^{1/2} \times \left[y_1\left(1 - \frac{743}{1050t} + \frac{3x_1}{7t^2}\right) - y_2\left(\frac{1}{6} - \frac{221}{600b} + \frac{x_2}{14t^2}\right)\right] \tag{B.7}$$

and

$$B_d(s') = \left(\frac{a\lambda}{5}\right)^2\left(\frac{12}{\pi b^3}\right)^{1/2}\left[y_1\left(\frac{20}{9} - \frac{2257}{350b} + \frac{12}{7}\frac{z_1}{b^2}\right) + y_2\left(\frac{5}{18} + \frac{3089}{700b} + \frac{2z_2}{7b^2}\right)\right] - \left(\frac{a\lambda}{5}\right)^2\left(\frac{3}{2\pi t^3}\right)^{1/2} \times \left[y_1\left(\frac{20}{9} - \frac{2257}{700t} + \frac{3z_1}{7t^2}\right) + y_2\left(\frac{5}{18} + \frac{3089}{1400t} + \frac{z_2}{14t^2}\right)\right] \tag{B.8}$$

where $t = \lambda s'$.

Appendix C. Derivation of $m_{VH}^{(2)}$

Here we derive eq 5.23 starting from eq 5.15. We first use eq 3.2 in order to express $m_{VH}^{(2)}$ in terms of tangent unit vectors and obtain

$$m_{VH}^{(2)}(|s_1 - s_2|) = \int_{s_1}^{s_2} ds_i \int_{s_1}^{s_2} ds_j\ (\hat{j}\cdot\hat{u}_1\hat{u}_1\cdot\hat{k})(\hat{j}\cdot\hat{u}_2\hat{u}_2\cdot\hat{k})(\hat{q}\cdot\hat{u}_i)(\hat{q}\cdot\hat{u}_j) \tag{C.1}$$

We evaluate the average indicated in the above equation. This is done in two steps. The first one involves evaluating the conditional average of $\hat{u}_1\hat{u}_1$ for a fixed $\hat{u}_i$ and the conditional average of $\hat{u}_2\hat{u}_2$ relative to $\hat{u}_j$. To do this we use the fact that i and j represent points on the molecular axis intermediate between 1 and 2. We thus initially postulate that the ordering of these points on the molecular axis is $1 \le i \le j \le 2$. The results for other allowed orders of indices are obtained from the ones obtained for this case. Using this ordering and the distribution function of eq 5.20, we find

$$\langle \hat{u}_1\hat{u}_1\rangle_{\hat{u}_i} = \tfrac{1}{3}\mathbf{1}(1 - e^{-6\lambda|s_1 - s_i|}) + \hat{u}_i\hat{u}_i e^{-6\lambda|s_1 - s_i|} \tag{C.2}$$

An equivalent expression, with subscripts 2 and j replacing, respectively, 1 and i is obtained for $\langle \hat{u}_2\hat{u}_2\rangle_{\hat{u}_j}$. Thus we have

$$\langle (\hat{j}\cdot\hat{u}_1\hat{u}_1\cdot\hat{k})(\hat{j}\cdot\hat{u}_2\hat{u}_2\cdot\hat{k})(\hat{q}\cdot\hat{u}_i)(\hat{q}\cdot\hat{u}_j)\rangle = \langle (\hat{j}\cdot\hat{u}_i\hat{u}_i\cdot\hat{k})(\hat{j}\cdot\hat{u}_j\hat{u}_j\cdot\hat{k})(\hat{q}\cdot\hat{u}_i)(\hat{q}\cdot\hat{u}_j)\rangle \times \exp[-6\lambda(|s_1 - s_i| + |s_2 - s_j|)] \tag{C.3}$$

The average indicated on the right-hand side of this expression now involves only unit vectors $\hat{u}_i$ and $\hat{u}_j$ and may be evaluated using $g(\hat{u}_i,\hat{u}_j)$, with the result

$$\langle (\hat{j}\cdot\hat{u}_1\hat{u}_1\cdot\hat{k})(\hat{j}\cdot\hat{u}_2\hat{u}_2\cdot\hat{k})(\hat{q}\cdot\hat{u}_i)(\hat{q}\cdot\hat{u}_j)\rangle = \frac{1}{105}\exp[-12\lambda|s_i - s_j|] + \frac{1}{525}[3\exp(-12\lambda|s_i - s_j|) + 7\exp(-2\lambda|s_i - s_j|)]\cos^2\frac{\alpha}{2}$$

where we have used eq 5.8 for q. Integration of this expression over s_i and s_j yields eq 5.23.

References and Notes

(1) (a) Berne, B. J.; Pecora, R. "Dynamic Light Scattering"; Wiley-Interscience: New York, 1976. (b) Yamakawa, H. "Modern Theory of Polymer Solutions"; Harper and Row: New York, 1971. (c) Flory, P. J. "Statistical Mechanics of Chain Molecules"; Wiley-Interscience: New York, 1969.
(2) Ladanyi, B. M.; Keyes, T. *Mol. Phys.* **1981**, *42*, 501.
(3) Ladanyi, B. M.; Keyes, T. *Mol. Phys.* **1979**, *37*, 1809; *J. Chem. Phys.* **1982**, *76*, 2047. Ladanyi, B. M. *Ibid.* **1982**, *76*, 4303.
(4) Justification for this approximation was explained in detail in ref 2. The approximation is equivalent to the Burgers approximation used in hydrodynamics (see: Burgers, J. M. "Second Report on Viscosity and Plasticity of the Amsterdam Academy of Sciences"; Nordemann Publishing Co.: Amsterdam, 1938; Chapter III).
(5) Dung, M. H.; Ladanyi, B. M., unpublished.
(6) Gradsteyn, I. S.; Ryzhik, I. M. "Table of Integrals, Series, and Products"; Academic Press: New York, 1980.
(7) (a) Gobush, W. Ph.D. Thesis, Dartmouth College, 1970 (unpublished). (b) Gobush, W.; Yamakawa, H.; Stockmayer, W. H.; Magee, W. S. *J. Chem. Phys.* **1972**, *57*, 2839.
(8) Landau, L. D.; Lifshitz, E. M. "Electrodynamics of Continuous Media"; Pergamon Press: Oxford, U.K., 1960.
(9) Bottcher, T. J. F. "Theory of Electric Polarization"; Elsevier: Amsterdam, 1973.
(10) Huglin, M. B. In "Light Scattering from Polymer Solutions"; Huglin, M. B., Ed.; Academic Press: London, 1972.
(11) Debye, P. *J. Appl. Phys.* **1944**, *15*, 338. Ewart, R. H.; Roe, C. P.; Debye, P.; McCartney, J. R. *J. Chem. Phys.* **1946**, *14*, 687. Debye, P. *J. Phys. Colloid Chem.* **1947**, *51*, 18.
(12) Arpin, M.; Strazielle, C.; Weill, G.; Benoit, H. *Polymer* **1977**, *18*, 262.
(13) Nagai, K. *Polym. J.* **1972**, *3*, 67, 563.
(14) Peterlin, A.; Stuart, H. A. *Z. Phys.* **1939**, *112*, 1, 129. For a review of the current literature on this subject, see: Tricot, M.; Houssier, C. In "Polyelectrolytes"; Frisch, K. C.; Klempner, D.; Patsis, A. V., Eds.; Technomic Publishing Co.: Westport, CT, 1976. For a discussion of experimental evidence for the breakdown of this approximation, see: Meeten, G. H. *J. Chem. Soc., Faraday Trans. 2* **1979**, *75*, 1405.
(15) Fortelny, I. *J. Polym. Sci., Polym. Phys. Ed.* **1974**, *12*, 2319.
(16) Jernigan, R. L.; Flory, P. J. *J. Chem. Phys.* **1967**, *54*, 1351. Patterson, G. D.; Flory, P. J. *J. Chem. Soc., Faraday Trans. 2* **1972**, *68*, 1098. Bothorel, P.; Fourche, G. *Ibid.* **1973**, *69*, 441.
(17) Parkhurst, H. J.; Jonas, J. *J. Chem. Phys.* **1975**, *63*, 2705.
(18) Ladanyi, B. M.; Dung, M. H., to be submitted.